sustainability

MDPI

Article

Daily Average Wind Power Interval Forecasts Based on an Optimal Adaptive-Network-Based Fuzzy Inference System and Singular Spectrum Analysis

Zhongrong Zhang [1,*], Yiliao Song [2,†], Feng Liu [2,†] and Jinpeng Liu [3]

1 School of Mathematics and Physics, Lanzhou Jiaotong University, No. 88, West Annin Road, Anning District, Lanzhou 730070, China
2 School of Statistics, Dongbei University of Finance and Economics, No. 217, Jianshan Street, Shahekou District, Dalian 116025, China; Songyl13@lzu.edu.cn (Y.S.); Liuf13@lzu.edu.cn (F.L.)
3 Geological Natural Disaster Prevention Research Institute, Gansu Academy of Sciences, No. 229, Dinxi South Road, Chengguan District, Lanzhou 730070, China; liujp03@126.com
* Correspondence: gslzzhangzhr@126.com; Tel./Fax: +86-931-493-8625
† These authors contributed equally to this work.

Academic Editor: Andrew Kusiak
Received: 13 October 2015; Accepted: 26 January 2016; Published: 29 January 2016

Abstract: Wind energy has increasingly played a vital role in mitigating conventional resource shortages. Nevertheless, the stochastic nature of wind poses a great challenge when attempting to find an accurate forecasting model for wind power. Therefore, precise wind power forecasts are of primary importance to solve operational, planning and economic problems in the growing wind power scenario. Previous research has focused efforts on the deterministic forecast of wind power values, but less attention has been paid to providing information about wind energy. Based on an optimal Adaptive-Network-Based Fuzzy Inference System (ANFIS) and Singular Spectrum Analysis (SSA), this paper develops a hybrid uncertainty forecasting model, IFASF (Interval Forecast-ANFIS-SSA-Firefly Alogorithm), to obtain the upper and lower bounds of daily average wind power, which is beneficial for the practical operation of both the grid company and independent power producers. To strengthen the practical ability of this developed model, this paper presents a comparison between IFASF and other benchmarks, which provides a general reference for this aspect for statistical or artificially intelligent interval forecast methods. The comparison results show that the developed model outperforms eight benchmarks and has a satisfactory forecasting effectiveness in three different wind farms with two time horizons.

Keywords: average wind power; interval forecasts; optimal subtractive clustering method; ANFIS; SSA; Model comparison

1. Introduction

1.1. Motivation

Given the important environmental advantages of renewable energy sources, the installation of wind power plants has significantly increased in most industrialized countries to comply with international environmental agreements [1]. The total installed capacity of wind power in China has reached 96.37 GW, a share of approximately 27% of the global capacity, due to the historically high installation of the new wind power capacity of 19.81 GW in 2014 [2]. Moreover, a renewable-energy-oriented power system was proposed as the fundamental aim of China's energy transformation during the APEC (Asia-Pacific Economic Cooperation) Conferences [3]. The current policy trend to move China toward having a larger fraction of its energy portfolio devoted to renewable

energy resources puts additional strain on the energy industry, because these sources have, to date, been less predictable than traditional generation sources. There is a need for advanced prediction techniques to integrate wind energy into the electrical power grid in a manner that benefits both TSOs (Transmission System Operators), which are obliged to maintain large power reserves in gas or oil generators, and IPPs (Independent Power Producers), which usually participate in short-term electricity markets by providing bids or making bilateral contracts for their wind power production [4,5].

1.2. Literature Review and Background

The inherently intermittent nature and stochastic non-stationarity of wind sources bring great levels of uncertainty to system operators [6]. Therefore, precise wind forecasts are of primary importance to solve operational, planning and economic problems in the growing wind power scenario [6–8]. For thorough discussions regarding the quantification of the economic benefits of accurate forecasts for power systems, we refer to [4] and the references therein. Current wind power forecasting research has been divided into point forecasts (also called deterministic predictions) [9–11] and uncertainty forecasts [12,13]. Deterministic forecasts enable the delivery of specific amounts of wind power at a future time and focus on reducing the prediction error [14]. In contrast, it is essential to decision-making processes and electricity market trading strategies [15] that uncertainty forecasts provide uncertainty information for system operators to manage the wind power generation of wind farms [13]. However, compared to the deterministic prediction skills, uncertainty forecasting technologies still require further advanced research [12], given that these two aspects of wind power forecasts are of equal importance to the integration of wind energy in power systems [12–14,16].

The existing approaches published in the literature with respect to wind power uncertainty forecasts can be separated into three categories: probabilistic forecasts [17], skill forecasts (commonly in the form of prediction risk indices) [18] and scenarios [19]. This paper mainly focuses on probabilistic forecasts, which express both the generation and forecast error of wind power for a given look-ahead time by quoting some of its quantiles, using prediction intervals, or, alternatively, providing the entire predictive density [17,18]. The effectiveness of the probabilistic method appears to be partly affected by low quality forecasts of the deterministic power prediction model due to an inevitable point forecast process before uncertainty estimation models [14,18]. A simple and novel interval forecast to directly estimate the upper or lower limits of wind speeds has been proposed in [20]. This type of uncertainty prediction avoids an accumulated error of deterministic forecasts because of the absence of point prediction or distribution simulation; therefore, it is applied in this paper.

With the interval forecast method mentioned above, prediction works transform into two equivalent point forecast problems regarding the estimation of the upper or lower limits for wind power. Three branches of point forecast techniques in the literature are summarized as follows. (1) The first branch is mathematical modeling approaches including statistical and artificial intelligence methods, which mainly establish the relation between prediction data and historical power data sets [21]. (2) The second branch is physical approaches, which are mostly based on NWP (Numeric Weather Prediction). An NWP model is usually characterized as a set of three main components: the "dynamical" core, dealing with the basic set of equations of the adiabatic inviscid flow; the "physics" pack, which includes a variable number of equations representing processes such as radiation, phase transitions, convection, or turbulence; and the data assimilation code [22]. Despite estimating the wind power value, physical methods simulate an atmospheric system to output a detailed forecast of the state of the atmosphere at a given time, such as the local wind speed, by using physical laws and based on these outputs the corresponding power generation can be calculated [1,23]. For example, Zhao *et al.* developed a wind power forecast system based on the NWP which combines the Kalman filter and artificial neural networks to improve the forecast accuracy [5]. (3) of the third branch combines both approaches, which adds meteorological variables, mainly wind speed and direction, as additional input data to the mathematical models [1,24]. Although NWP performs the best in forecasting precision over a long time frame among these methods, it requires more physical information [25] and is therefore

too complex to implement [7]. Moreover, NWP may not be the best choice regarding short prediction horizons (3–6 h ahead) [7].

The wind power industry needs forecasts over time scales ranging from a few minutes to several years for a wide range of applications, including turbine blade pitch control, conversion systems control, load scheduling, maintenance scheduling, and resource planning [8]. Among those, a short-term wind power forecast (from 1 h up to 72 h) [23] is essential for the integration of wind farms because both bidding and contracting market sides require the quantity of produced electricity [26]. Current research of short-term power forecasts, especially physical forecasts, is focusing on deterministic minutes or hourly wind energy values. In fact, decision-makers in electrical power systems generally require more information than the values of a single point with respect to electricity market management and trading strategies [15]. Beyond the need for forecasting the detailed production of tomorrow's wind power for each time point, there is a basic need for forward awareness of deterministic or uncertain future daily wind power, *i.e.*, knowledge of the average or total quantity for TSOs and IPPs to schedule the spinning reserve capacity and manage the grid operations in advance.

1.3. Aim and Contributions

To forecast the uncertainty information of future wind power values, this paper develops a hybrid model, IFASF, based on singular spectrum analysis (SSA), an adaptive-network-based fuzzy inference system (ANFIS), subtractive clustering, the firefly algorithm and a simple interval forecast method. Compared to the traditional interval forecast model, which usually involves a deterministic estimation before the interval forecasts, the proposed model can directly predict the upper or lower limits of daily average wind power values, thus avoiding the accumulated error of point prediction or distribution simulation. Moreover, the forecast accuracy of 25 weeks of wind power prediction values in Gansu, China, has been validated as satisfactory via comprehensive comparisons between methods. Therefore, IFASF is suggested as an effective model to provide the basic uncertainty information of the average interval for tomorrow's wind power. Our main contributions are as follows.

(1) SSA is applied for de-noising daily average wind power;
(2) The neighborhood radius of the subtractive clustering algorithm is optimized by the firefly algorithm;
(3) Based on the optimal neighborhood radius, SSA and ANFIS, we develop a hybrid interval forecasting method, IFASF, for daily average wind power;
(4) An extensive comparison of the Autoregressive Integrated Moving Average Model (ARIMA), Back Propagation Neural Network (BPNN), Extreme Learning Machine (ELM), ANFIS, ARIMA-SSA, BPNN-SSA, ELM-SSA, ANFIS-SSA and IFASF lays a strong foundation for future research regarding interval forecasts of average wind power;
(5) IFASF outperforms other benchmarks when forecasting 70% and 80% intervals of the mean wind power.

This paper is organized as follows: Section 2 will introduce the main methodology used in this article; Section 3 gives the proposed model's detailed procedures and its mathematical expression; Section 4 utilizes IFASF to forecast 70%, 80% and 90% intervals of the average wind power and analyzes the forecasting effectiveness of the developed model and other benchmarks; and Section 5 summarizes the main results of this paper.

2. Methodology

This paper directly outputs interval limits by training upper or lower limits of historic wind power values by a hybrid model of SSA [27], ANFIS [28], FA [29] and an Interval Forecast (IF) [20]. All of these four models will be summarized in this section, and the detailed information of the hybrid model is presented in Section 3. To avoid symbol confusion in these four methods, the parameters are listed in Table 1.

Table 1. Symbol table.

Method	Symbol	Description
	α	Confidence level
SSA	C	A real number determined by actual situation
	τ	Time lag
	M	Embedding dimension
	M'	Assumed upper limit of the noisy part
ANFIS	$\{a_i, b_i, c_i\}$	Premise parameters
	$\{p_i, q_i, r_i\}$	Consequent parameters
Subtractive clustering	r	Neighborhood radius
	$\eta*$	a constant larger than 1
FA	γ	distance between fireflies
	a	light absorption coefficient
	I_0	light intensity
	δ	randomization parameter

2.1. Interval Forecasts

A simple but efficient interval forecasting method in [20] is introduced in this paper, in which the upper and lower limits are trained by two parallel sets. Let *x(t)* be a wind power series, and then the basic principles are as follows:

Definition 2.1.1: For a specified $C \in R$ and $wp_i \in [0, C]$, $L(wp, \mathrm{i}, \alpha)$ is its lower limit at the confidence level of α, while $U(wp, \mathrm{i}, \alpha)$ is the upper limit.

$$\begin{cases} L(wp, \mathrm{i}, \alpha) = wp_i + \alpha \times C \\ U(wp, \mathrm{i}, \alpha) = wp_i + \alpha \times C \end{cases} \quad \alpha \in (0, 1) \tag{1}$$

Definition 2.1.2: The evaluation of $L(wp, \mathrm{i}, \alpha)$ or $U(wp, \mathrm{i}, \alpha)$ at a target point t_0 is defined as:

$$\begin{cases} \hat{L}(wp, t_0, \alpha) = \hat{F}_L\left(L(wp, t_0 - 1, \alpha), L(wp, t_0 - 2, \alpha), \ldots, L(wp, t_0 - \tau, \alpha)\right) \\ \hat{U}(wp, t_0, \alpha) = \hat{F}_U\left(U(wp, t_0 - 1, \alpha), U(wp, t_0 - 2, \alpha), \ldots, U(wp, t_0 - \tau, \alpha)\right) \end{cases} \tag{2}$$

where τ represents the time lag, and $\hat{F}_L$ or $\hat{F}_U$ is a mapping of evaluations from the historic series.

2.2. Singular Spectrum Analysis

Based on principal component analysis (PCA), SSA, since first introduced into nonlinear dynamics [27], has been broadly used as a data-analysis method in digital signal processing [30]. Applications of SSA in the wind area are rare and mainly focus on large gap-filling in solar wind [31] and pre-filters for further meteorology studies [32]. In this paper, SSA is suggested as a filtering technique for wind power values before forecasts. The steps are as follows:

Build the trajectory matrix: Based on Takens's theorem [33], wind power time series $\{wp_i\}, i = 1, 2, \ldots N$ can be embedded into a phase space $X^{M \times (N-M+1)}$. Its trajectory matrix X at lag 1 with an embedding dimension M can be written as follows:

$$X = \begin{pmatrix} wp_1 & wp_2 & \cdots & wp_{N-M+1} \\ wp_2 & wp_3 & \cdots & wp_{N-M+2} \\ \vdots & & \cdots & \vdots \\ wp_M & wp_{M+1} & \cdots & wp_N \end{pmatrix} \tag{3}$$

Singular Value Decomposition: The lagged-covariance matrix [30] *Cov* of X is defined as Equation (4).

$$Cov = \begin{pmatrix} c(0) & c(1) & \dots & c(M-1) \\ c(1) & c(0) & \dots & c(M-2) \\ \vdots & & \dots & \vdots \\ c(M-1) & c(M-2) & \dots & c(0) \end{pmatrix} \tag{4}$$

where $c(\tau)$ is the covariance of X at lag τ.

$$c(\tau) = \frac{1}{N-\tau} \sum_{i=1}^{N-\tau} wp_i wp_{i+\tau} \tag{5}$$

The eigenvalues of Cov, $\lambda_1 \geqslant \lambda_2 \geqslant \cdots \geqslant \lambda_k \geqslant 0$ which are obviously non-negative, are sorted in descending order and the corresponding eigenvectors are denoted by E_j^k which is also called the empirical orthogonal functions. Based on that, the principal component a_i^k is defined as follows:

$$a_i^k = \sum_{j=1}^{M} wp_{i+j} E_j^k, \quad 0 \leqslant i \leqslant N-M \tag{6}$$

The sorted square-root of λ_i, $\left\{\sqrt{\lambda_i} \middle| \sqrt{\lambda_i} \geqslant \sqrt{\lambda_{i+1}}\right\}$. which is also called the singular values, forms the singular spectrum for the system [34]. Generally, noisy signals are considered to have smaller singular values.

Restructure: For known principal components a_i^k and empirical orthogonal functions E_j^k [30,34], the original time series can be restructured as Definition 2.2.2.

Definition 2.2.2: Given the original time series wp_i, its de-noised series $SSA\left(wp_i, M, M'\right)$ is defined as follows:

$$SSA\left(wp_i, M, M'\right) = \begin{cases} \frac{1}{i} \sum_{j=1}^{i} a_{i-j+1}^k \left(wp_i, M, M'\right) E_j^k \left(wp_i, M, M'\right) & 1 \leqslant i \leqslant M-1 \\ \frac{1}{M} \sum_{j=1}^{M} a_{i-j+1}^k \left(wp_i, M, M'\right) E_j^k \left(wp_i, M, M'\right) & M \leqslant i \leqslant N-M+1 \\ \frac{1}{N-i+1} \sum_{j=i-N+M}^{i} a_{i-j+1}^k \left(wp_i, M, M'\right) E_j^k \left(wp_i, M, M'\right) & N-M+2 \leqslant i \leqslant N \end{cases} \tag{7}$$

where M denotes the embedding dimension, and M' denotes the assumed upper limit of the noisy part. Then $a_{i-j+1}^k \left(wp_i, M, M'\right)$ are principle components, and $E_j^k \left(wp_i, M, M'\right)$ are empirical orthogonal functions in Equation (7).

2.3. Adaptive-Network-Based Fuzzy Inference System with Subtractive Clustering

This paper introduces a subtractive clustering technique when applying the ANFIS to estimate the lower and upper limits of wind power. In this section, a brief overview of ANFIS is discussed and is followed by a description of the principle of the subtractive clustering algorithm.

2.3.1. Adaptive-Network-Based Fuzzy Inference System

ANFIS is introduced to compensate for the disability of conventional mathematical tools to address uncertain systems, such as human knowledge and reasoning processes. Jang [28] restructured FISs with two contributions: proposing a standard method for transforming ill-defined factors into identifiable rules of FIS and using an adaptive network to tune the membership functions. This restructuring yields the ANFIS, which has been validated for its availability in the wind energy area [35,36]. We assume the system contains two fuzzy if-then rules [37], two inputs (x and y) and one output (z), and the processes of ANFIS are described in Figure 1.

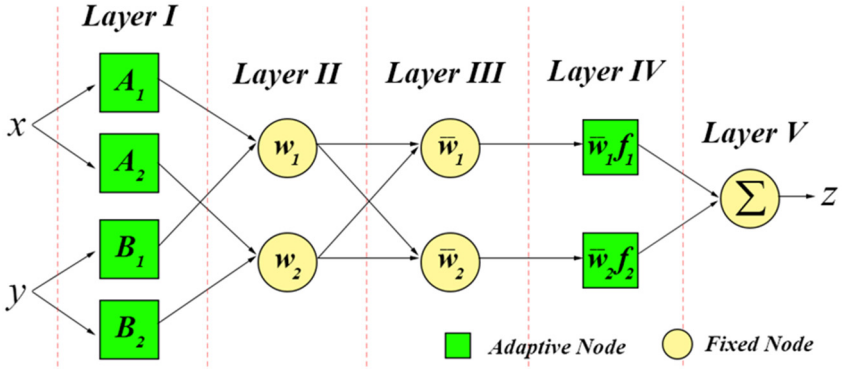

Figure 1. There are five processes, or layers, in an ANFIS architecture, where circles are fixed nodes without parameters and squares represent adaptive nodes whose parameters are determined by training data and a gradient-based learning procedure [28].

Layer I: A certain input x is mapped to a fuzzy set O_i^1 for every node i by the member functions μ_{A_i}, which is usually bell-shaped with a parameter set $\{a_i, b_i, c_i\}$, as is y.

$$O_i^1 = \mu_{A_i}(x), \text{ where} \mu_{A_i}(x) = \frac{1}{1+\left[\left(\frac{x-c_i}{a_i}\right)^2\right]^{b_i}}, \text{ or } \mu_{A_i}(x) = \exp\left\{-\left(\frac{x-c_i}{a_i}\right)^2\right\} \quad (8)$$

Layer II: In this layer, each circle node performs the connection "AND" and multiplies inputs as well as sends the product out:

$$O_i^2 = \omega_i = \mu_{A_i}(x) \times \mu_{B_i}(y) \quad (9)$$

Layer III: Every circle node in this layer calculates a normalized firing strength, namely a ratio of the i^{th} rule's firing strength to the sum of all the rules' firing strengths:

$$O_i^3 = \overline{\omega}_i = \frac{\omega_i}{\sum_i \omega_i} \quad (10)$$

Layer IV: Assume the rules of this system are as follows [37]:
Rule 1: If x is A_1 and y is B_1, then $f_1 = p_1 x + q_1 y + r_1$
Rule 2: If x is A_2 and y is B_2, then $f_2 = p_2 x + q_2 y + r_2$
Then, the outputs of the adaptive nodes in this layer are computed by:

$$O_i^4 = \overline{\omega}_i f_i = \overline{\omega}_i (p_i x + q_i y + r_i) \quad (11)$$

Layer V: The overall output is the weighted average of all incoming signals:

$$O_i^5 = \sum_i \overline{\omega}_i f_i = \frac{\sum_i \omega_i f_i}{\sum_i \omega_i} \quad (12)$$

Particularly, in this case,

$$O_i^5 = \overline{\omega}_1 f_1 + \overline{\omega}_2 f_2 = (\overline{\omega}_1 x) p_1 + (\overline{\omega}_1 y) q_1 + \overline{\omega}_1 r_1 + (\overline{\omega}_2 x) p_2 + (\overline{\omega}_2 y) q_2 + \overline{\omega}_2 r_2 \quad (13)$$

To clearly describe the computational process of ANFIS, an example is introduced as follows: in a well-trained ANFIS with two fuzzy if-then rules and a bell-shaped member function, given a specified input $(L(wp, t-2, \alpha), L(wp, t-1, \alpha))$, each of them can be mapped into two values in Layer I. For the condition of $x = L(wp, t-2, \alpha)$, these two values are $A_1 = 1/\left\{1+\left[((x-c)/a)^2\right]^b\right\}$ and $A_2 = \exp\left\{-((x-c)/a)^2\right\}$, and for $y = L(wp, t-1, \alpha)$, these two values are $B_1 = 1/\left\{1+\left[((y-c)/a)^2\right]^b\right\}$ and $B_2 = \exp\left\{-((y-c)/a)^2\right\}$. With A_1, A_2, B_1, B_2, ω_i can

be computed such that $\omega_1 = A_1 \times B_1$ and $\omega_2 = A_2 \times B_2$. In Layer III, $\overline{\omega}_i$ can be computed easily by Equation (10). In Layer IV, based on the two if-then rules, $f_1 = p_1 x + q_1 y + r_1$ and $f_2 = p_2 x + q_2 y + r_2$ and the output of Layer IV is $\overline{\omega}_i f_i$. The output of Layer V, which is the output of the ANFIS, is a simple sum of the output of Layer IV, namely $\hat{L}(wp, t, \alpha) = \overline{\omega}_1 f_1 + \overline{\omega}_2 f_2$. To achieve a desired input-output mapping, the parameters are updated according to given training samples and a gradient-based learning procedure is described in [28].

2.3.2. Subtractive Clustering Algorithm

Layer I of ANFIS involves determining the membership functions (MFs), and, generally, it is hard for a visualization technique to reach the necessary precision, especially when the number of rules exceeds three [38]. Therefore, it is highly desirable that an automatic model identification method be realized by a data set rather than an expert's experience. Clustering skills are often introduced here, and this paper applies the subtractive clustering algorithm.

For the subtractive clustering method, each data point x_i is considered a potential cluster center; then, based on the density of its neighbor points, final clusters are determined by the likelihood of each cluster center [39].

For data points $\{x_i\}$ in the M-Dimension space, the likelihood P_i of each potential cluster center x_i is defined as below:

$$P_i = \sum_{j=1}^{m} exp\left(-\frac{||x_i - x_j||^2}{(r/2)^2}\right) \tag{14}$$

where $||x_i - x_j||$ denotes the Euclidean distance between x_i and its neighbors x_j, and r is a positive constant defining a neighborhood radius. The first cluster center $P_{c_1}^*$ is chosen as the point c_1 which has the highest likelihood value. For the next center, the likelihood value is computed after subtracting the effect of the former cluster center, as follows:

$$P_i = P_i - P_{c_1}^* exp\left(-\frac{||x_i - x_{c_1}||^2}{(r'/2)^2}\right) \tag{15}$$

where $r' = \eta^* r$ and η^* is a constant larger than one to avoid cluster centers being in too-close proximity [40]. Similarly, the second cluster center c_2 has a larger likelihood value than the other points. Generally, cluster centers are iteratively selected by Equation (16) until the stopping criteria are achieved.

$$c_k = \underset{i}{arg\,max}\left\{P_i \middle| P_i = P_i - P_{c_{k-1}}^* exp\left(-||x_i - x_{c_{k-1}}||^2/\left(r'/2\right)^2\right)\right\} \tag{16}$$

Definition 2.3.1. Given an initial neighborhood radius $r \sim$ U(a, b), a and b are fixed, and the estimation y_i of x_i by ANFIS with the subtractive clustering method can be defined as below [28]:

$$y_i = Model(x_i) \tag{17}$$

This map's *Model* is defined as

$$Model(x_i; r) = ANFIS(\text{TrainSet}, r) \tag{18}$$

where TrainSet = $\{x_i, Y_i\}$, and Y_i is the actual value of x_i.

Remark: In Definition 2.3.1, *Model*(x_i;r) is a map from x_i to y_i and is relative to r, which is a random variable. When r is a constant, we can express this model simply using *Model*(x_i).

2.4. Firefly Algorithm

The firefly algorithm (FA), developed by Xin-she Tang [29], is enlightened by the natural behaviors of the firefly. A firefly moves together with other partners because of its tendency to move toward a brighter flash, which is determined by the light intensity of the other fireflies and the distance between them. Assuming three idealized rules are established [29], FA can be summarized as follows.

Definition 2.4.1: $I(\gamma)$ of a firefly is the visible light intensity with γ distance from other fireflies:

$$I(\gamma) = I_0 e^{-a\gamma^2} \tag{19}$$

where I_0 is the light intensity of the firefly itself and a the light absorption coefficient.

Definition 2.4.2: $\beta(\gamma)$ is the attractiveness of a firefly with r distance from other fireflies:

$$\beta(\gamma) = \beta_0 e^{-a\gamma^2} \tag{20}$$

where $\beta(\gamma)$ represents the maximum attractiveness.

Definition 2.4.3: Firefly i will be attracted by a brighter firefly j with movement determined by

$$x_i(t+1) = x_i(t) + \beta\left(x_j(t) - x_i(t)\right) + \delta\left(rand - \frac{1}{2}\right) \tag{21}$$

where δ is the randomization parameter.

Based on the rules and definitions above, FA can be summarized in Algorithm 1.

Algorithm 1. Firefly Algorithm.

Input: $\boldsymbol{x} = (x_1, x_2, \ldots, x_d)^T$, **Objective function**: $f(x)$
Generate initial population of fireflies $\boldsymbol{x}_i$ $(i = 1, 2, \ldots, n)$
While $t < MaxIteration$
  For $i = 1 : n$
    For $j = 1 : i$
      If $I_j > I_i$

$$x_i(t+1) = x_i(t) + \beta\left(x_j(t) - x_i(t)\right) + \delta\left(rand - \frac{1}{2}\right)$$

      Else

$$x_i(t+1) = x_i(t)$$

      End If
  End For
End While

3. Introduction to the Proposed Model

Let N be a set of positive integers, and suppose that $W = (wp_1, wp_2, \ldots, wp_n)$, which is the mean wind power series, and $wp_i \in [0, C]$, where $n \in$ N and C denotes the installed capacity of the wind farm (it should be clarified that this paper only collects wind power data and there is no other additional data used, which indicates that the input data of the models is only wind power data). The main steps of the proposed model are as demonstrated below.

Step 1. Divide W into $W_{train} = (wp_1, wp_2, \ldots, wp_m)$ and $W_{test} = (wp_{m+1}, wp_2, \ldots, wp_n)$, and they both satisfy

$$W_{train} \bigcup W_{test} = W \text{ and } W_{train} \bigcap W_{test} = \varnothing \tag{22}$$

Step 2. According to Definition 2.2.2, let

$$Ws_{train} = SSA(W_{train}, 10, 4) \tag{23}$$

Step 3. Let d, $nt \in$ N, $X \subseteq \mathrm{R}^d$ be the input space constructed by elements in W_{train} and $Y \subseteq$ R be the output space constructed by elements in Ws_{train}. Let

$$\mathrm{TA} = (x_i, y_i)_{i=1}^{nt} \tag{24}$$

where TA is a family of random samples in which $x_i \in X$ and $y_i \in Y$.

Step 4. Let ntr, $nvd \in [1, nt) \subset \mathrm{N}$, and generate nvd random numbers r_i ($i = 1, 2, \ldots, nvd$) that obey a normalized Gaussian distribution $\mathrm{N}(0,1)$. Let

$$I_{vd} = \{\lfloor nt \times r_i \rfloor \,|r_i, i = 1, 2, \ldots, nvd\} \subset \mathrm{N} \tag{25}$$

Thus, we have

$$\mathrm{Vd} = (x_i, y_i)_{i \in I_{vd}} \tag{26}$$

and

$$\mathrm{TRN} = \{(x_i, y_i) \in \mathrm{TA} \,|i \in [1, nt] \text{ and } i \notin I_{vd}\} \tag{27}$$

Step 5. Let $\alpha \in (0, 1]$ be a parameter to calculate the upper and lower bounds of interval forecasts, and we have

$$\mathrm{Vd\_U}(\alpha) = \{(x_i, \alpha \times C + y_i) \,|(x_i, y_i) \in \mathrm{Vd}\} \tag{28}$$

$$\mathrm{Vd\_L}(\alpha) = \{(x_i, -\alpha \times C + y_i) \,|(x_i, y_i) \in \mathrm{Vd}\} \tag{29}$$

and

$$\mathrm{TRN\_U}(\alpha) = \{(x_i, \alpha \times C + y_i) \,|(x_i, y_i) \in \mathrm{TRN}\} \tag{30}$$

$$\mathrm{TRN\_L}(\alpha) = \{(x_i, -\alpha \times C + y_i) \,|(x_i, y_i) \in \mathrm{TRN}\} \tag{31}$$

Step 6. Adjust y_i of Vd_U, Vd_L, TRN_U and TRN_L using the following equation:

$$y_i = \begin{cases} 0, & y_i < 0 \\ 1, & y_i > C \\ \dfrac{y_i}{C}, & otherwise \end{cases}, y_i \in \mathrm{Vd\_U, Vd\_L, TRN\_U \text{ and } TRN\_L} \tag{32}$$

Step 7. According to Definition 2.3.1, build and train two basic ANFISs with TRN_U, TRN_L and $r \sim \mathrm{U}(0.03,0.3)$, which is a neighborhood radius of the subtractive clustering method, and we express both of them by

$$Model\_U(x_i; r) = ANFIS(\mathrm{TRN\_U}, r) \tag{33}$$

and

$$Model\_L(x_i; r) = ANFIS(\mathrm{TRN\_L}, r) \tag{34}$$

where *Model_U* and *Model_L* are maps from X to Y, and their parameters are relative with r.

Step 8. Generate a loss function:

$$J(r) = \sum_{i=1}^{nvd} \left(\sqrt{(Model\_U(x_i^U; r) - y_i^U)^2} + \sqrt{(Model\_L(x_i^L; r) - y_i^L)^2} \right) \tag{35}$$

where $(x_i^U, y_i^U) \in$ Vd_U and $(x_i^L, y_i^L) \in$ Vd_L.

Step 9. Let the objective function of FA be

$$\min_r J(r) \tag{36}$$

where $r \sim \mathrm{U}(0.03, 0.3)$, and denote the best r obtained by this objective function by $r_{best} \in [0.03,0.3]$.

Step 10. Obtain the IFASF model and express it by

$$IFASF\_U(x_i) = ANFIS(\mathrm{TRN\_U}, r_{best}) \tag{37}$$

and

$$IFASF\_L(x_i) = ANFIS(\mathrm{TRN\_L}, r_{best}) \tag{38}$$

Remark: Step 1 to Step 10 specifically demonstrate IFASF using a mathematical process, and they show how to utilize one wind power time series to train the IFASF and obtain an upper bound and lower bound. Figure 2 shows the flowchart of IFASF with a specific sample.

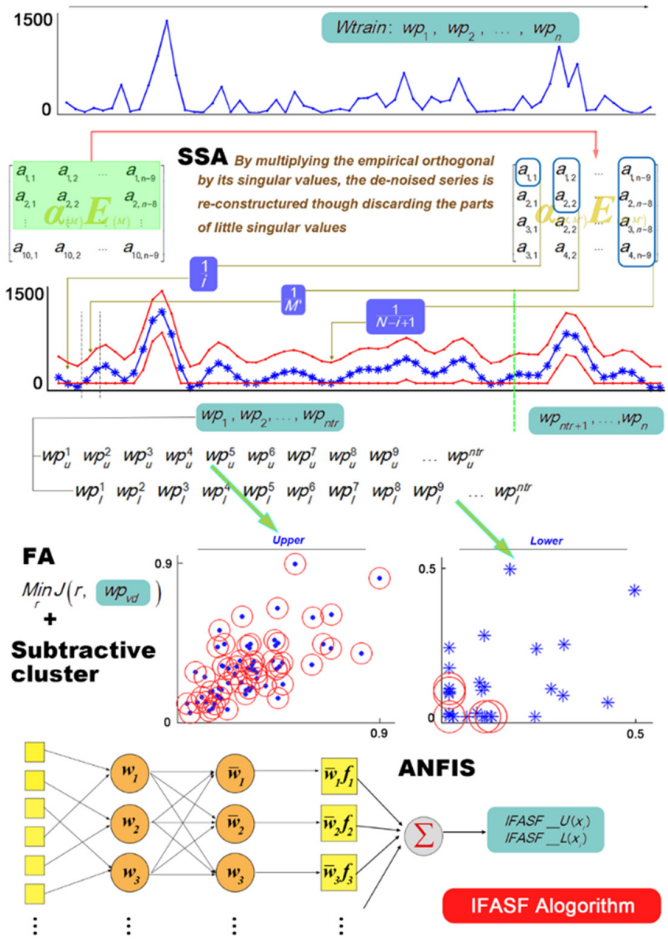

Figure 2. Flowchart of the developed model with a specific sample.

4. Numerical Results and Analysis

In this section, detailed forecasting results and corresponding analyses will be demonstrated by tables and figures, and comparisons between other models will also be specifically illustrated.

4.1. Data Collections, Forecasting Principles and Parameter Settings

We collected wind power data from three different wind farms (denoted by W1, W2 and W3) in Gansu Province in 2013 and randomly selected 25 weeks of data (175 days from each wind farm) to validate the effectiveness of the developed model. The main forecasting principles are demonstrated as follows.

- Two previous wind power points of the forecasting point were used to construct input spaces of a basic ANFIS.
- Training samples of the IFASF were constructed for the week to be validated using the previous 60 days of wind power data.
- The proposed model was re-trained after it had provided seven days of forecasting results.

Parameters were set as follows: η and μ of CWC (the definition of CWC and its parameters are listed in the Appendix) of 0.5 and 75%, respectively.

4.2. Interval Forecasting Results

For the purpose of testing the forecasting effectiveness of each model, this paper prepares five experiments with data from three different wind farms to illustrate each model's forecasting consequence and the priority of the developed model.

4.2.1. Experiment I

This experiment shows W1's interval forecasting effectiveness of ANFIS, ANFIS-SSA and IFASF, which is evaluated by IFCP and IFNAW (the definition of IFCP, IFNAW and its parameters are listed in the Appendix) in Table 2. A 70% interval forecast is more meaningful than other interval forecasts because IFCP of the 70% interval forecast is higher than that of the 80% and 90% interval forecasts, indicating that the mean wind power is unstable data and it is difficult to forecast its interval which covers the actual values. Although the interval of average wind power data is hard to forecast, ANFIS-SSA and IFASF still give satisfactory results because their IFCPs are more than 70% when used to forecast a 70% interval of wind power. Alternately, ANFIS only has a 65.14% successful coverage percentage in the same situation, which suggests that the method developed by SSA and FA indeed improves the coverage percentage. From the average values of each column, IFCPs of IFASF are 40%, 62.29% and 76%, which are higher than the 37.14%, 56.57% and 72% obtained with ANFIS-SSA and the 30.29%, 52% and 65.14% obtained with ANFIS. For the IFNAW criteria, IFASF also outperforms other models when forecasting the 70% wind power interval. From the perspective of the number of time that each method reaches a 100% coverage percentage, ANFIS has one week in which the IFCP is 100%, the IFCP of ANFIS-SSA peaks at 100% five times, and the developed model, IFASF, has eight weeks in which the forecasting interval covers all of the actual mean wind power points, which shows that IFASF is a better model to calculate wind power points' upper bounds and lower bounds. Specifically, the ANFIS model obtains the highest IFCP when forecasting the 70% interval in week 11 and the lowest IFCP in week 2 for the 90% interval forecast. Similarly, the forecasting results in week 2 of ANFIS-SSA are also invalidated when they are used to calculate the 90% upper and lower bounds for wind power points. The IFCP of the model developed by SSA peaks at 100% five times when forecasting the 80% interval in week 25 and the 70% interval in weeks 13, 17, 24 and 25. For the IFASF model, its IFCP peaks at 100% eight times: in week 9 for the 70% interval forecast, week 11 for the 70% interval forecast, week 13 for the 80% and 70% interval forecasts, week 17 for the 70% interval forecast, week 24 for the 70% interval forecast and week 25 for the 80% and 70% interval forecasts. Additionally, the developed model obtains the worst IFCP when forecasting the 90% interval of week 2. To illustrate the information in this table, Figure 3 is constructed to show the merits of the developed model. In Figure 3a, the IFCPs are divided into three categories, which are ranges from 0% to 50%, 50% to 80% and 80% to 100%, and it is obvious that the IFCPs of IFASF belong to (80%~100%) 12 times, which are the highest among these three models, and they belong to (50%~80%) and (0%~50%) 10 times and three times, respectively, which are the lowest among ANFIS, ANFIS-SSA and IFASF (see the table in the sub-figure of Figure 3). Figure 3b–d are histograms of the IFCPs of the three models, and the right portion of the IFCP axis indicates a higher IFCP. Thus, the IFASF model's IFCPs are higher than those of the other models, indicating that SSA and FA actually improve the interval forecasting ability of ANFIS and show a good pre-process and optimal effectiveness for randomly selected weeks. Figure 3e,f illustrate the context of Table 2 and they also show that the proposed model has a good performance for 70%, 80% and 90% interval forecasts.

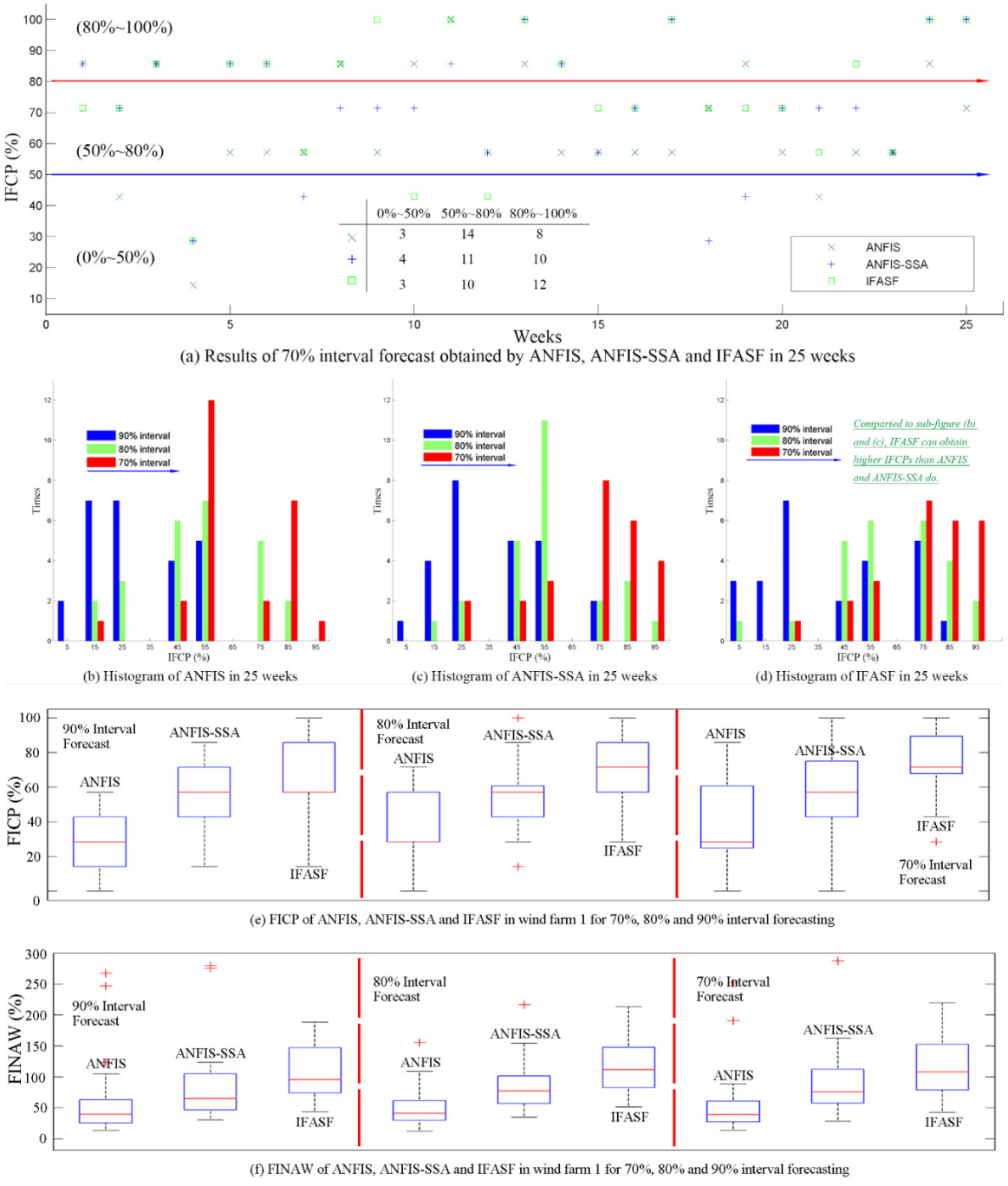

(a) Results of 70% interval forecast obtained by ANFIS, ANFIS-SSA and IFASF in 25 weeks

(b) Histogram of ANFIS in 25 weeks

(c) Histogram of ANFIS-SSA in 25 weeks

(d) Histogram of IFASF in 25 weeks

(e) FICP of ANFIS, ANFIS-SSA and IFASF in wind farm 1 for 70%, 80% and 90% interval forecasting

(f) FINAW of ANFIS, ANFIS-SSA and IFASF in wind farm 1 for 70%, 80% and 90% interval forecasting

Figure 3. Histograms and plots of the main results of the interval forecast of 25 weeks in W1.

Table 2. Main interval forecasting results of ANFIS, ANFIS-SSA and IFASF in W1.

Weeks	ANFIS						ANFIS-SSA						IFASF					
	IFCP (%)			IFNAW (%)			IFCP (%)			IFNAW (%)			IFCP (%)			IFNAW (%)		
	90.00%	80.00%	70.00%	90.00%	80.00%	70.00%	90.00%	80.00%	70.00%	90.00%	80.00%	70.00%	90.00%	80.00%	70.00%	90.00%	80.00%	70.00%
1	42.86	85.71	85.71	105.07	275.77	393.68	71.43	57.14	85.71	109.43	147.66	335.51	85.71	85.71	71.43	191.02	287.31	386.50
2	0.00	14.29	42.86	15.81	31.36	43.50	0.00	57.14	71.43	12.48	35.00	51.61	0.00	42.86	71.43	25.42	43.16	58.68
3	57.14	85.71	85.71	267.57	465.26	619.34	57.14	85.71	85.71	155.64	411.33	514.84	71.43	85.71	85.71	252.09	465.03	509.18
4	14.29	14.29	14.29	26.83	46.57	67.54	42.86	42.86	28.57	16.32	38.33	64.97	14.29	57.14	28.57	23.86	70.06	75.06
5	28.57	57.14	57.14	31.22	64.51	92.32	28.57	57.14	85.71	34.81	77.42	119.98	71.43	71.43	85.71	39.74	71.52	97.17
6	42.86	57.14	57.14	53.53	92.26	134.44	28.57	57.14	85.71	51.26	114.86	178.47	57.14	71.43	85.71	60.74	107.38	150.58
7	0.00	42.86	57.14	24.30	40.76	56.62	14.29	42.86	42.86	13.86	51.19	78.55	0.00	0.00	57.14	22.36	42.35	62.99
8	14.29	71.43	85.71	61.09	116.99	168.30	14.29	14.29	71.43	61.03	92.08	137.46	28.57	71.43	85.71	71.34	130.05	160.08
9	42.86	42.86	57.14	29.50	58.16	94.26	57.14	57.14	71.43	65.33	81.89	111.91	28.57	42.86	100.00	39.50	76.20	108.21
10	14.29	28.57	85.71	30.89	56.08	90.33	28.57	28.57	71.43	41.52	97.75	138.11	28.57	28.57	42.86	25.73	47.66	75.27
11	57.14	42.86	100.00	41.80	78.32	122.65	57.14	42.86	85.71	29.16	79.54	137.64	28.57	85.71	100.00	60.37	111.30	149.23
12	14.29	28.57	57.14	13.77	30.60	50.11	57.14	57.14	57.14	27.29	49.66	64.96	14.29	42.86	42.86	14.25	28.58	43.02
13	42.86	71.43	85.71	88.70	104.78	184.63	42.86	85.71	100.00	76.56	139.94	191.12	57.14	100.00	100.00	64.04	116.80	161.46
14	57.14	57.14	57.14	16.77	42.92	54.18	14.29	71.43	85.71	34.46	61.51	87.81	71.43	85.71	85.71	31.25	72.51	94.26
15	28.57	57.14	57.14	35.02	64.42	95.95	42.86	42.86	57.14	43.36	76.63	102.96	42.86	57.14	71.43	34.60	73.86	107.23
16	14.29	57.14	57.14	40.11	65.05	89.27	28.57	57.14	71.43	47.49	87.24	118.71	28.57	71.43	71.43	38.69	80.90	107.83
17	28.57	71.43	57.14	123.65	123.65	123.65	57.14	85.71	100.00	95.70	216.81	213.21	0.00	57.14	100.00	76.35	138.55	197.47
18	57.14	42.86	71.43	36.76	61.57	88.82	14.29	42.86	28.57	32.42	57.29	82.20	14.29	42.86	71.43	38.42	58.40	115.12
19	28.57	71.43	85.71	42.39	79.05	111.73	28.57	28.57	42.86	35.56	70.96	98.38	57.14	57.14	71.43	52.12	75.97	108.20
20	28.57	28.57	57.14	23.50	46.81	76.41	28.57	57.14	71.43	46.04	70.74	94.32	57.14	71.43	71.43	28.20	55.17	86.45
21	14.29	42.86	42.86	23.05	44.76	63.10	42.86	57.14	71.43	23.66	46.45	66.92	28.57	42.86	57.14	23.31	47.81	79.55
22	28.57	57.14	57.14	71.18	107.62	140.72	28.57	57.14	71.43	37.50	73.17	102.43	42.86	57.14	85.71	42.04	80.83	123.22
23	14.29	42.86	57.14	59.15	84.89	109.01	28.57	57.14	57.14	30.59	57.02	83.23	28.57	57.14	57.14	32.27	68.70	77.87
24	57.14	71.43	85.71	246.94	279.60	309.60	71.43	71.43	100.00	51.82	80.93	123.90	71.43	71.43	100.00	51.34	90.52	122.65
25	28.57	57.14	71.43	40.44	97.40	188.15	42.86	100.00	100.00	75.54	154.32	209.33	71.43	100.00	100.00	88.92	162.63	219.78
Std.	18.13	19.73	18.93	64.95	98.42	127.65	18.90	19.55	20.82	32.69	77.29	99.79	25.75	22.92	20.08	53.66	91.66	103.63
Average	30.29	52.00	65.14	61.96	102.37	142.73	37.14	56.57	72.00	49.95	98.79	140.34	40.00	62.29	76.00	57.12	104.13	139.08

4.2.2. Experiment II

In this experiment, interval forecasting results of ARIMA, BPNN, ELM, ARIMA-SSA, BPNN-SSA, ELM-SSA, ANFIS, ANFIS-SSA and IFASF will be demonstrated and compared in W1. The ARIMA model is an extension of the regular ARMA model and involves three essential parts of auto-regression, moving average and integration in order to model the serial correlations of a stochastic process [41]. ELM is a single hidden-layer feedforward neural network, which randomly chooses the input weights and analytically determines the output weights [42]. As one of the famous machine learning algorithms, BPNN is also employed as a benchmarking comparison model [43]. The ARIMA-SSA, BPNN-SSA and ELM-SSA models all use SSA pre-processed data to train ARIMA, BPNN and ELM, respectively (when testing the effectiveness of BPNN and ELM, they both use actual data to construct the input space). Table 3 shows the main interval forecasting results of nine models by three criteria, and CWC's parameters are mentioned in Section 4.1. From this table, IFASF obviously has a higher mean IFCP than the other models, and only the developed model meets the 75% standard set in the CWC criteria, which is a combined index to evaluate the effectiveness of interval forecasts. Additionally, for the CWC criteria, IFASF has the lowest values for 70% and 80% interval forecasts. From the perspective of the interval forecasts' utility, 90% interval forecasts are invalidated for the reason that the highest IFCP of these models is 40%, which is far from the standard 75% (possibly because of the stochastic nature of wind and wind power). Thus, we will mainly discuss each model's effectiveness when forecasting 70% and 80% intervals in this section. For ARIMA and ARIMA-SSA models, the highest IFCP peaks at 61.14% using ARIMA pre-processed by SSA for 70% interval forecasts, and the lowest CWC is 860.18, which appears when forecasting an 80% interval using ARIMA-SSA. From the boxplot of ARIMA and ARIMA-SSA's interval forecasts shown in Figure 4, the SSA method develops the original ARIMA to obtain a better forecasting performance than the original one (CWC provides the main criteria to evaluate the model's effectiveness). The BPNN model is a classical artificial neuron network (ANN) and has been used to solve many forecasting problems. In this paper, BPNN utilizes historical data to train its parameters and directly obtains the upper bounds and lower bounds.

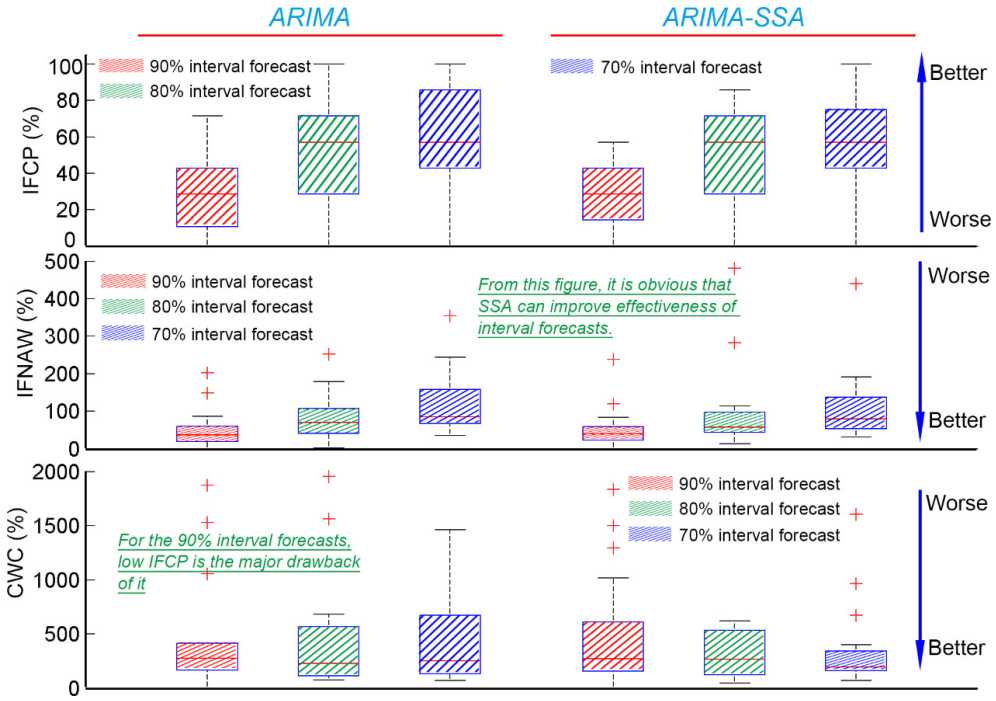

Figure 4. Boxplot of the results of ARIMA and ARIMA-SSA by three criteria in W1 (for the purpose of convenient comparisons among these models, the CWC axis is limited below 2000 and there are many points that are not shown in the CWC part of Figure 4).

Table 3. Main interval forecasting results of the nine models in W1.

Model	Criteria								
	Mean IFCP (%)			Mean IFNAW (%)			Mean CWC (%)		
	90.00%	80.00%	70.00%	90.00%	80.00%	70.00%	90.00%	80.00%	70.00%
ARIMA	30.29	52.00	60.57	47.21	101.74	143.35	806.61	1443.84	1922.82
BPNN	29.71	53.71	57.14	53.58	102.82	142.30	569.97	659.20	597.81
ELM	29.14	49.71	62.86	53.90	99.08	138.60	590.70	464.48	410.68
ANFIS	30.29	52.00	65.14	61.96	102.37	142.73	648.38	372.92	358.90
ARIMA-SSA	27.43	50.29	61.14	47.09	87.33	124.99	918.05	860.18	1402.35
BPNN-SSA	36.57	50.29	71.43	54.57	93.93	133.92	447.79	430.42	309.64
ELM-SSA	36.00	54.29	71.43	52.46	93.62	132.74	431.81	380.32	483.80
ANFIS-SSA	37.14	56.57	72.00	49.95	98.79	140.34	415.39	384.66	293.10
IFASF	40.00	62.29	76.00	57.12	104.13	139.08	508.16	321.53	261.04

From the perspective of comparisons between BPNN and BPNN-SSA, BPNN-SSA's CWCs are 447.79, 430.42 and 309.64, which are lower than the 569.97, 659.20 and 597.81 obtained by BPNN, indicating that SSA lays a strong foundation to improve the interval forecasting effectiveness. It is valuable to note that the CWC criteria decrease by nearly 48% from the original model to the model pre-processed by SSA. Figure 5 shows boxplots of the results of BPNN and BPNN-SSA by IFCP, IFNAW and CWC. Similarly, SSA can improve the 70% interval forecasting abilities of BPNN from this figure. For the contents in Figure 6, the forecasting abilities of ELM are also improved using SSA. Thus, for the benchmark models, SSA can always improve the original models' forecasting effectiveness, especially for the 70% interval forecasts. Then, comparisons among these nine methods will be demonstrated by two categories: the original models and models pre-processed by SSA. Table 3 shows that ELM, a new ANN which was recently developed, outperforms BPNN, a classical ANN, when forecasting 80% and 70% intervals and that ANFIS has the best performance among BPNN, ELM, ANFIS and ARIMA when forecasting 70% and 80% intervals, suggesting that ANFIS is the best model among these basic models. Each model's forecasting ability changes when utilizing SSA to pre-process original data. In particular, ANFIS-SSA is not the best method when forecasting the 80% interval, and ELM-SSA does not outperform BPNN-SSA for 70% interval forecasts, thus indicating that SSA has a different effect on different models and cannot guarantee that model M-SSA will outperform model N-SSA if model M outperforms model N (M or N is ARIMA, BPNN, ELM or ANFIS in this paper).

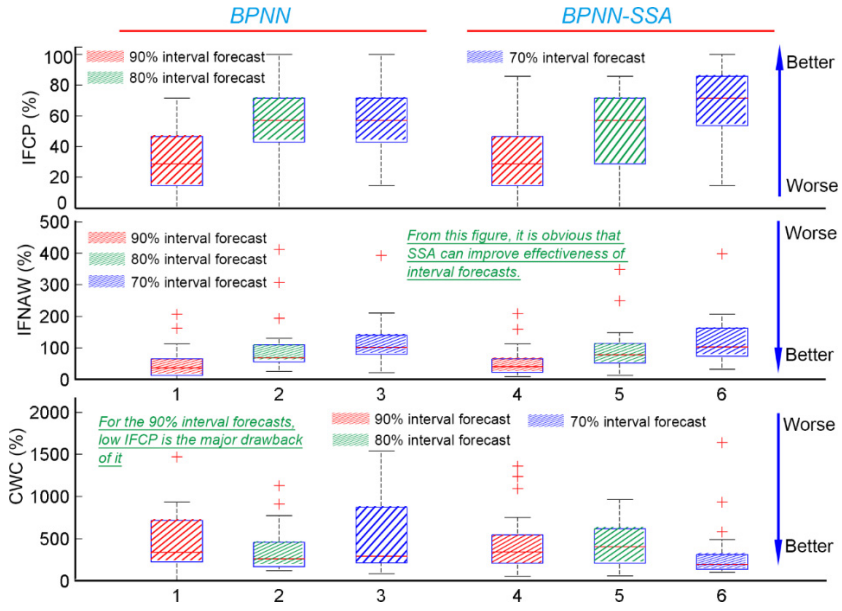

Figure 5. Boxplot of the results of BPNN and BPNN-SSA by three criteria in W1.

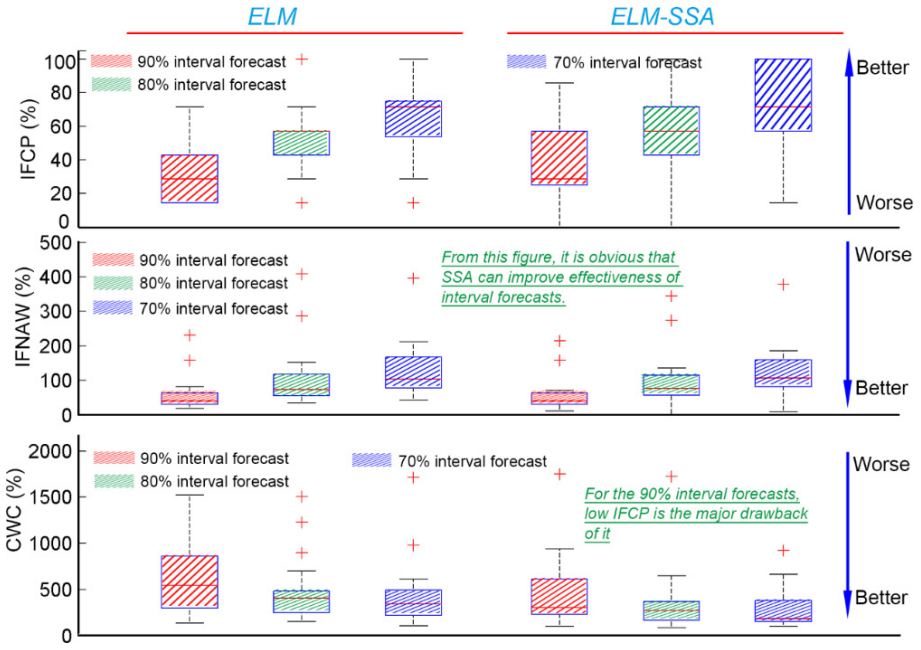

Figure 6. Boxplot of the results of ELM and ELM-SSA by three criteria in W1.

However, no matter which model (basic models or models pre-processed by SSA) is considered, the IFASF model is still the best interval forecasting model because its IFCP is closer to the standard IFCP of 75% than the IFCPs of the other models. In Figure 7, which presents the boxplot of each model when forecasting 70% and 80% intervals, the blue line represents the 75th percentile of CWC of 80% interval forecasts and the red line represents the 75th percentile of CWC of 70% interval forecasts. It is obvious that the red line's points are almost lower than those of the blue line, suggesting that 70% interval forecasts have better performance than 80% interval forecasts. From the perspective of the models' forecasting effectiveness, IFASF apparently outperforms other models no matter which criteria are considered to evaluate interval forecasts (such as the median of CWC, the 75th percentile of CWC or the average value of CWC). Thus, from the above analysis of forecasting results, the developed model, IFASF, is the best interval forecasting model for mean wind power points.

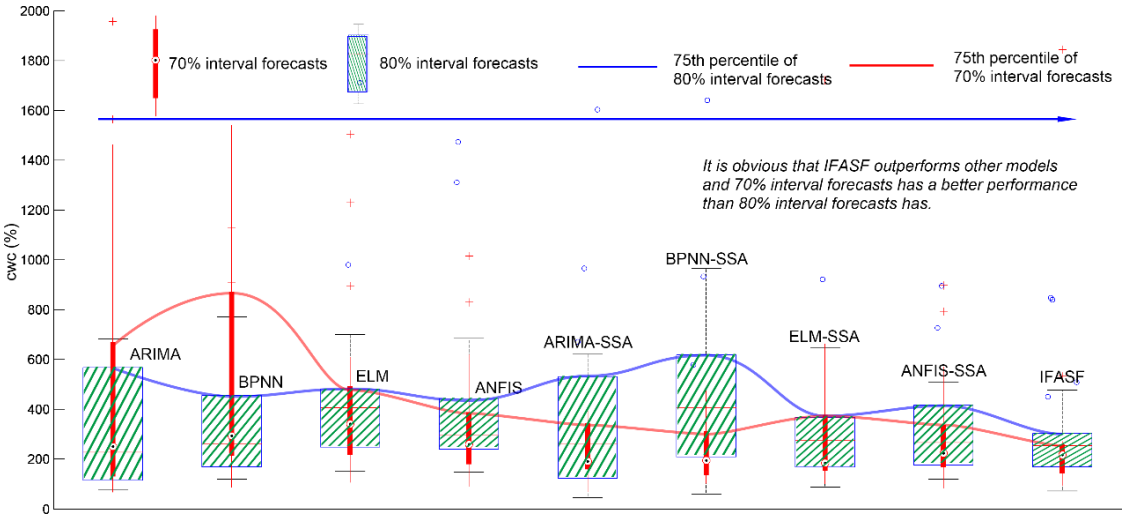

Figure 7. Boxplot of each model when forecasting 70% and 80% intervals in W1.

4.2.3. Experiment III

Initially, this experiment will show the interval forecasting effectiveness of ANFIS, ANFIS-SSA and IFASF in W2, which are evaluated by IFCP and IFNAW in Table 4. It is apparent that the 70% interval forecast is more meaningful than the other interval forecasts because the IFCP of the 70% interval forecast is higher than that of the 80% and 90% interval forecasts, which are similar to the results obtained in W1. ANFIS-SSA and IFASF provide satisfactory results because their IFCPs are more than 70% when they are used to forecast 70% intervals of wind power. However, ANFIS has only a 63.43% successful coverage percentage in the same situation, which means that SSA and FA play important roles in improving the coverage percentage. From the average values of each column, the IFCPs of IFASF are higher than those of ANFIS-SSA and ANFIS when forecasting 70% and 80% intervals. For the IFNAW criteria, IFASF also outperforms other models when forecasting 70% and 80% wind power intervals. From the perspective of high coverage percentage, ANFIS has nine weeks whose IFCPs are over 80%, the IFCP of ANFIS-SSA is more than 80% 22 times and the developed model, IFASF, also has 22 weeks in which the forecasting interval covers 80% of the actual mean wind power points, which shows that ANFIS-SSA and IFASF are better models to calculate the wind power points' upper bounds and lower bounds. Specifically, if IFCPs are divided into three categories that range from 0% to 50%, 50% to 80% and 80% to 100%, then it will be obvious that the IFCPs of IFASF belong to (80%~100%) 22 times, which is higher than those of ANFIS, and to (50%~80%) and (0%~50%) 31 and 22 times, respectively. In Figure 8a, the red and blue lines divide this figure into three parts, which represent the intervals (80%–100%), (50%–80%) and (0%–50%) of IFCP. Figure 8b,c illustrate the context of Table 4 and they indicate that the proposed model has higher FICPs than ANFIS and ANFIS-SSA have. From this figure and Table 4, it can be observed that IFASF outperforms ANFIS-SSA mainly because when their IFCPs belong to (0%–50%), the IFCPs of the developed model are higher than those of ANFIS-SSA, and IFASF outperforms ANFIS because IFASF has more points whose IFCPs are over 80% than ANFIS does.

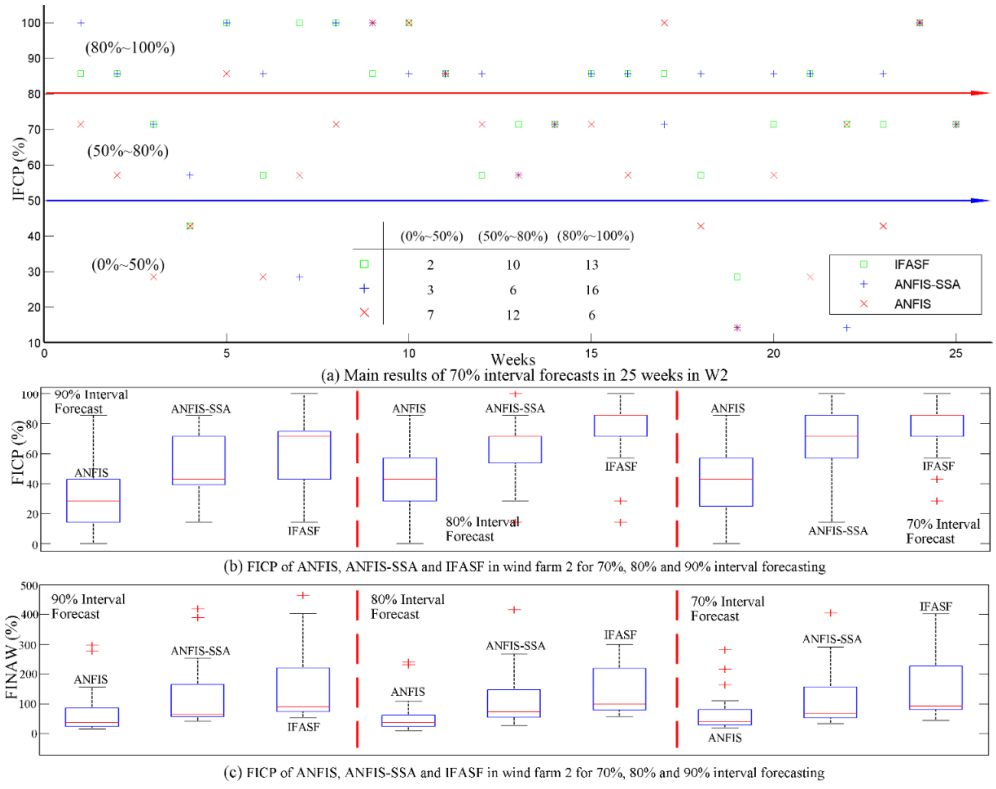

Figure 8. Main results of interval forecasts in 25 weeks in W2.

Table 4. Main interval forecasting results of ANFIS, ANFIS-SSA and IFASF in W2.

Weeks	ANFIS						ANFIS-SSA						IFASF					
	IFCP (%)			IFNAW (%)			IFCP (%)			IFNAW (%)			IFCP (%)			IFNAW (%)		
	90.00%	80.00%	70.00%	90.00%	80.00%	70.00%	90.00%	80.00%	70.00%	90.00%	80.00%	70.00%	90.00%	80.00%	70.00%	90.00%	80.00%	70.00%
1	57.14	57.14	71.43	43.83	56.29	64.59	28.57	85.71	100.00	14.08	31.78	57.12	57.14	85.71	85.71	20.10	34.06	45.32
2	42.86	42.86	57.14	35.49	62.19	90.90	57.14	71.43	85.71	47.05	91.81	123.56	28.57	71.43	85.71	31.51	72.06	103.27
3	14.29	14.29	28.57	39.49	59.53	78.22	42.86	71.43	71.43	38.64	71.33	95.76	42.86	57.14	71.43	40.38	66.44	93.14
4	42.86	28.57	42.86	23.02	67.96	88.71	14.29	57.14	57.14	25.99	56.37	80.66	0.00	28.57	42.86	27.61	55.74	82.59
5	85.71	85.71	85.71	156.67	220.48	273.45	57.14	71.43	100.00	109.29	177.42	268.99	42.86	71.43	100.00	102.78	197.45	272.76
6	14.29	14.29	28.57	36.93	62.89	91.70	42.86	57.14	85.71	38.02	78.87	105.31	42.86	57.14	57.14	35.79	69.86	100.61
7	28.57	57.14	57.14	278.88	419.54	602.12	14.29	28.57	28.57	86.73	724.62	836.04	14.29	85.71	100.00	281.37	699.91	876.46
8	71.43	71.43	71.43	297.03	389.28	464.36	71.43	100.00	100.00	95.67	195.27	282.68	85.71	100.00	100.00	111.40	199.71	290.05
9	14.29	14.29	100.00	85.34	210.61	403.18	85.71	100.00	100.00	239.88	415.43	583.66	71.43	85.71	85.71	216.87	405.76	590.33
10	28.57	71.43	100.00	73.76	127.67	181.33	0.00	57.14	85.71	51.67	137.92	203.00	14.29	57.14	100.00	70.58	144.73	211.78
11	14.29	42.86	85.71	34.72	63.79	91.07	71.43	71.43	85.71	59.70	94.84	100.96	42.86	71.43	85.71	34.54	68.53	93.55
12	28.57	42.86	71.43	30.33	59.78	84.48	57.14	71.43	85.71	33.69	72.19	91.77	57.14	28.57	57.14	52.62	64.50	88.37
13	0.00	42.86	57.14	19.66	43.06	61.76	0.00	28.57	57.14	25.98	51.90	80.44	0.00	14.29	71.43	24.26	44.96	67.65
14	28.57	71.43	71.43	18.54	42.64	60.73	14.29	42.86	71.43	15.43	28.90	62.52	14.29	57.14	71.43	32.30	42.11	69.09
15	57.14	71.43	71.43	79.38	116.36	129.32	57.14	71.43	85.71	34.51	71.71	100.25	71.43	85.71	85.71	53.33	88.09	115.00
16	71.43	71.43	57.14	33.87	43.97	64.35	71.43	85.71	85.71	10.25	57.19	79.85	57.14	71.43	85.71	30.31	55.19	79.39
17	28.57	57.14	100.00	137.92	254.52	392.23	28.57	57.14	71.43	41.32	268.11	299.24	71.43	85.71	85.71	165.05	290.83	402.10
18	28.57	42.86	42.86	16.89	42.13	56.56	42.86	42.86	85.71	22.94	39.08	61.26	28.57	42.86	57.14	21.26	45.11	67.49
19	0.00	57.14	14.29	725.70	1327.80	1624.52	85.71	14.29	14.29	231.58	687.59	1269.39	57.14	85.71	28.57	676.17	632.02	900.32
20	28.57	42.86	57.14	22.69	60.95	93.88	28.57	42.86	85.71	41.38	80.82	112.60	28.57	42.86	71.43	42.29	76.77	111.66
21	28.57	28.57	28.57	17.50	44.11	54.16	28.57	71.43	85.71	28.42	50.68	70.35	14.29	57.14	85.71	29.39	52.22	71.86
22	0.00	57.14	71.43	26.25	64.58	88.88	57.14	57.14	14.29	20.35	50.36	78.29	57.14	71.43	71.43	28.14	54.38	82.10
23	14.29	14.29	42.86	47.84	67.05	89.84	28.57	71.43	85.71	33.05	73.89	96.56	28.57	57.14	71.43	46.15	59.22	86.32
24	42.86	85.71	100.00	92.56	150.75	204.38	28.57	71.43	100.00	71.11	126.95	192.58	42.86	85.71	100.00	74.98	137.58	189.84
25	14.29	42.86	71.43	41.90	65.75	103.01	57.14	71.43	71.43	38.07	62.45	87.93	57.14	71.43	71.43	39.78	72.48	92.92
Std.	22.96	21.85	24.43	150.94	264.07	327.65	24.74	21.03	24.65	58.99	187.40	283.65	23.44	21.46	18.44	137.94	178.59	239.98
Average	31.43	49.14	63.43	96.65	164.95	221.51	42.86	62.86	76.00	58.19	151.90	216.83	41.14	65.14	77.14	91.56	149.19	207.36

In the second part of Experiment III, the interval forecasting results of ARIMA, BPNN, ELM, ARIMA-SSA, BPNN-SSA, ELM-SSA, ANFIS, ANFIS-SSA and IFASF will be demonstrated and compared (these models have already been briefly introduced in Experiment 2). Table 5 shows the main interval forecasting results of the nine models by three criteria. IFASF has higher mean IFCPs than the other models, and only the developed model and ANFIS-SSA meet the 75% standard set in the CWC criteria, which is a combined index to evaluate the effectiveness of interval forecasts. Similar to the results of Experiment 2, for the CWC criteria, IFASF has the lowest values for 70% and 80% interval forecasts. From the perspective of the interval forecasts' utility, 90% interval forecasts are invalid because the highest IFCP of these models is 40%, which is far from the standard 75%. Thus, we will mainly discuss each models' effectiveness when forecasting 70% and 80% intervals in this section. For ARIMA and ARIMA-SSA models, the highest IFCP peak is 72.57% using ARIMA pre-processed by SSA for 70% interval forecasts, and the lowest CWC is 664.39, which appears when forecasting the 80% interval using ARIMA-SSA (this result is the same as the results in Experiment 2). From the boxplot of ARIMA and ARIMA-SSA's interval forecasts shown in Figure 9b, the SSA method develops the original ARIMA to obtain better forecasting performance than the original one (CWC is the main criteria to evaluate the model's effectiveness).

Table 5. Main interval forecasting results of nine models in W2.

Model	Criteria								
	Mean IFCP (%)			Mean IFNAW (%)			Mean CWC (%)		
	90.00%	80.00%	70.00%	90.00%	80.00%	70.00%	90.00%	80.00%	70.00%
ARIMA	32.57	60.00	72.57	71.00	145.45	180.91	1334.75	701.52	960.76
BPNN	30.29	46.29	58.29	72.09	135.75	184.44	915.82	1382.57	2488.25
ELM	22.29	45.71	65.71	73.37	130.93	195.32	1886.28	1980.08	1099.05
ANFIS	31.43	49.14	63.43	96.65	164.95	221.51	1948.50	864.88	1849.18
ARIMA-SSA	33.14	61.14	72.57	58.21	118.49	172.55	958.31	664.39	811.31
BPNN-SSA	32.00	54.86	72.00	60.44	124.56	220.45	1391.35	1031.07	1609.85
ELM-SSA	31.43	50.29	72.00	74.16	142.98	208.57	1332.14	2509.92	1045.54
ANFIS-SSA	42.86	62.86	76.00	58.19	151.90	216.83	445.89	1171.13	1721.56
IFASF	41.14	65.14	77.14	91.56	149.19	207.36	742.88	327.28	644.70

Comparing BPNN and BPNN-SSA, BPNN-SSA's CWCs are 1031.07 and 1609.85, which are lower than the 1382.57 and 2488.25 obtained by BPNN when forecasting 70% and 80% wind power intervals, respectively, indicating that SSA lays a strong foundation to improve the interval forecasting effectiveness. Notably, the CWC criteria decrease by nearly 30% from the original model to the model pre-processed by SSA. Figure 9c shows boxplots of the results of BPNN and BPNN-SSA by IFCP, IFNAW and CWC. Similarly, SSA can improve the 70% interval forecasting abilities of BPNN from this figure. For the contents in Figure 9f, the forecasting abilities of ELM are also improved using SSA. Thus, for the benchmark models, SSA can always improve their original models' forecasting effectiveness, especially for the 70% interval forecasts. Comparisons among these nine methods will be demonstrated by two categories: the original models and the models pre-processed by SSA. Table 5 shows that ELM only outperforms BPNN when forecasting the 70% interval and that there is not a single model that outperforms the other models for 70%, 80% and 90% interval forecasts among basic models. For models pre-processed by SSA, each model's forecasting abilities change when utilizing SSA to pre-process the original data. Specifically, ANFIS-SSA is the best method when forecasting 90% intervals and ARIMA-SSA is the best approach for 80% interval forecasts. This result also reflects the results obtained in Experiment 2 (SSA has a different effect on different models and cannot guarantee that model M-SSA will outperform model N-SSA if model M outperforms model N).

(a) Improved accuracy percentages of the ARIMA by the IFASF model.

Indexes	IFASF vs. ARIMA		
	90%	80%	70%
IFCP (%)	26.32%	8.57%	6.30%
CWC (%)	44.34%	53.35%	65.94%
Indexes	**IFASF v.s. ARIMA-SSA**		
	90%	80%	70%
IFCP (%)	24.14%	6.54%	6.30%
CWC (%)	22.48%	50.74%	59.66%

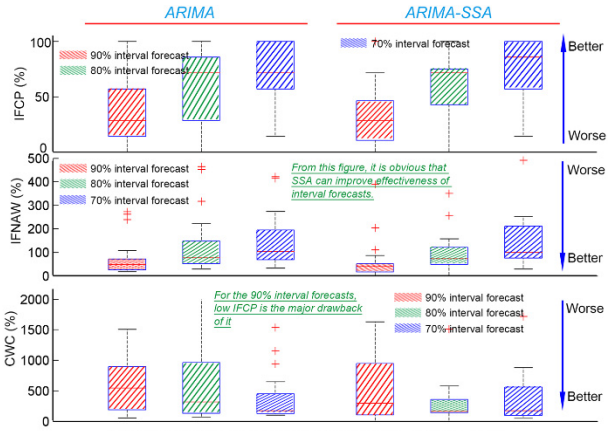

(b) Boxplot of results of ARIMA and ARIMA-SSA by three criteria in W2

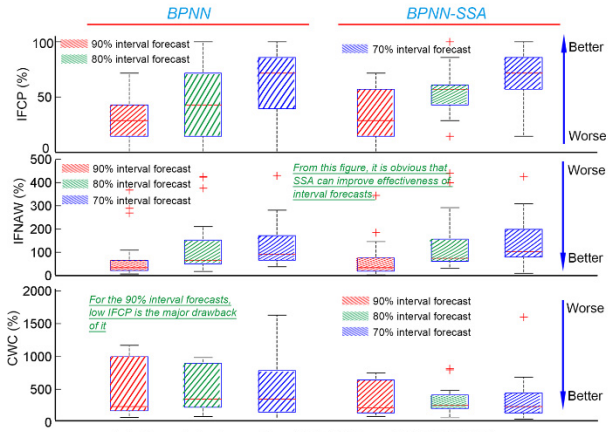

(c) Boxplot of results of BPNN and BPNN-SSA by three criteria in W2

(d) Improved accuracy percentages of the BPNN by the IFASF model.

Indexes	IFASF vs. BPNN		
	90%	80%	70%
IFCP (%)	35.85%	40.74%	32.35%
CWC (%)	18.88%	76.33%	86.85%
Indexes	**IFASF vs. BPNN-SSA**		
	90%	80%	70%
IFCP (%)	28.57%	18.75%	7.14%
CWC (%)	46.61%	68.26%	79.67%

(e) Improved accuracy percentages of the ELM by the IFASF model.

Indexes	IFASF vs. ELM		
	90%	80%	70%
IFCP (%)	84.62%	42.50%	17.39%
CWC (%)	60.62%	83.47%	70.22%
Indexes	**IFASF vs. ELM-SSA**		
	90%	80%	70%
IFCP (%)	30.91%	29.55%	7.14%
CWC (%)	44.23%	86.96%	68.70%

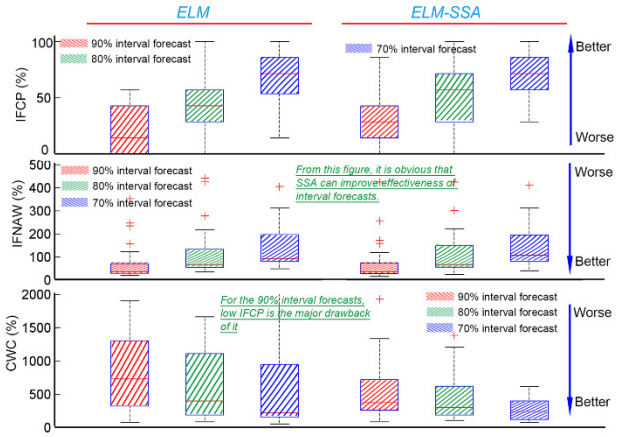

(f) Boxplot of results of ELMand ELM-SSA by three criteria in W2

Figure 9. Boxplots of the IFCPs of models and tables of the improved accuracy percentages of models by the IFASF model.

However, no matter which model (basic models or models pre-processed by SSA) is considered, the IFASF model is still the best interval forecasting model when forecasting 70% and 80% wind power intervals (see Figure 9a,d,e). In Figure 10, which presents a boxplot of each model when forecasting 70% and 80% intervals, the blue line represents the mean CWC of 80% interval forecasts, and the red line represents the mean CWC of 70% interval forecasts. From the perspective of models' forecasting effectiveness, IFASF apparently outperforms other models no matter which criteria are considered to

evaluate interval forecasts (such as the median of CWC, the 75th percentile of CWC or the average value of CWC). Thus, from the above analysis of the forecasting results, the developed model, IFASF, is the best interval forecasting model for mean wind power points in the W2 wind farm.

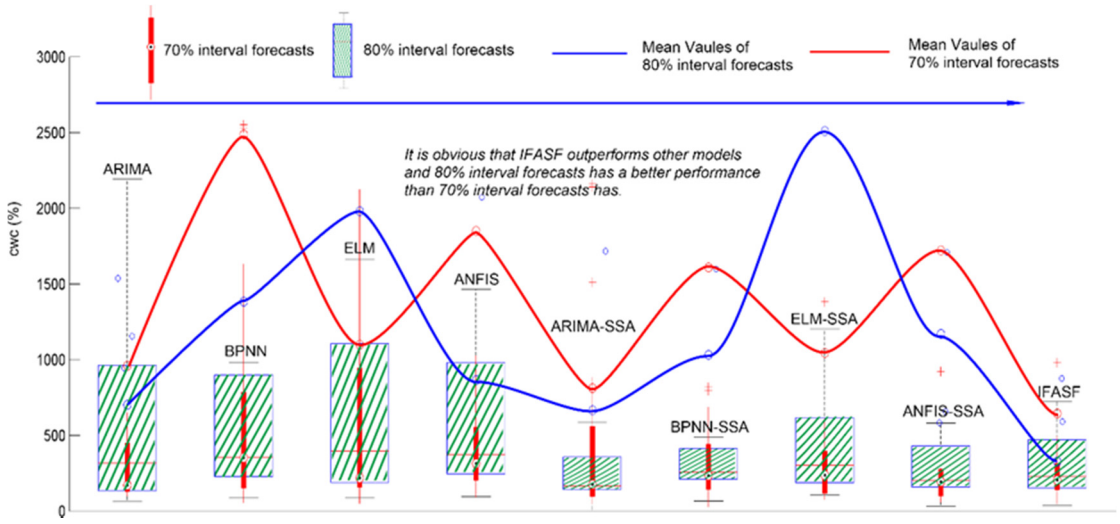

Figure 10. Boxplot of each model when forecasting 70% and 80% intervals in W2.

4.2.4. Experiment IV

W3's interval forecasting effectiveness of ANFIS, ANFIS-SSA and IFASF, which are evaluated by IFCP and IFNAW in Table 6, will be first shown in this experiment. From Table 6, the 70% interval forecast is still more meaningful than other interval forecasts because the IFCP of the 70% forecast is higher than that of the 80% and 90% interval forecast, indicating that the mean wind power is unstable data and that it is difficult to forecast its interval to cover its actual values again. Different from other wind farms, IFCPs of ANFIS, ANFIS-SSA and IFASF are more than 70% when forecasting 70% mean wind power intervals. Specifically, ANFIS has a 71.43% successful coverage percentage, ANFIS-SSA has a 78.29% successful coverage percentage and the IFCP of IFASF peaks at 85.14%. These results indicate that the SSA and FA play significant roles in improving the coverage percentage of the mean wind power. From the average values of each column, the IFCPs of IFASF for the 70%, 80%, and 90% interval forecasts are 44.57%, 66.86% and 85.14%, respectively, which are more than or equal to the 44.57%, 62.29% and 78.29% obtained by ANFIS-SSA and the 41.14%, 61.14% and 71.43% obtained by ANFIS. From the perspective of the highest coverage percentage, ANFIS has five weeks where IFCPs are 100%, the IFCP of ANFIS-SSA peaks at 100% 13 times, and the developed model, IFASF, has 18 weeks in which the forecasting interval covers all of the actual mean wind power points, illustrating that IFASF is a better model to calculate wind power points' upper bounds and lower bounds. Specifically, the ANFIS model obtains the highest IFCP when forecasting the 70% interval in weeks 11, 12, 21 and 25 and forecasting the 80% interval in week 11. The IFCP of the model developed by SSA peaks at 100% three times when forecasting the 80% interval in weeks 7, 10 and 24 and when forecasting the 70% interval in weeks 2, 7, 9, 12, 17, 19, 24 and 25. For the IFASF model, its IFCP peaks at 100% 18 times in week 2 for the 70% interval forecast, week 7 for the 70% and 80% interval forecasts, week 8 for the 70% interval forecast, week 9 for the 70% interval forecast, week 10 for the 70% and 80% interval forecasts, week 11 for the 70% and 80% interval forecasts, week 12 for the 70% interval, week 17th for 70% interval, week 18 for the 70% interval, week 19 for the 70%, 80% and 90% intervals, week 24 for the 70% and 80% intervals and week 25 for the 70% interval. For the purpose of illustrating information in this table, Figure 11 is constructed to show the merits of the developed model. In Figure 11a, the IFCPs are divided into three categories, which have ranges from 0% to 50%, 50% to 80% and 80% to 100%, and it is obvious that the IFCPs of IFASF or ANFIS-SSA belong to

(80%~100%) 17 times, which is higher than those of ANFIS, indicating that SSA and FA are helpful for improving forecasting effectiveness. Figure 11b–d, are histograms of the IFCPs of the three models, and being more to the right on the IFCP axis indicates a higher IFCP. Thus, the IFASF model's IFCPs are higher than other models' IFCPs, demonstrating that SSA and FA actually improve the interval forecasting ability of ANFIS and show a good pre-processing and optimal effectiveness for randomly selected weeks. Figure 11e,f illustrate the context of Table 6 and they also show that the proposed model is better than ANFIS and ANFIS-SSA for 70%, 80% and 90% interval forecasts.

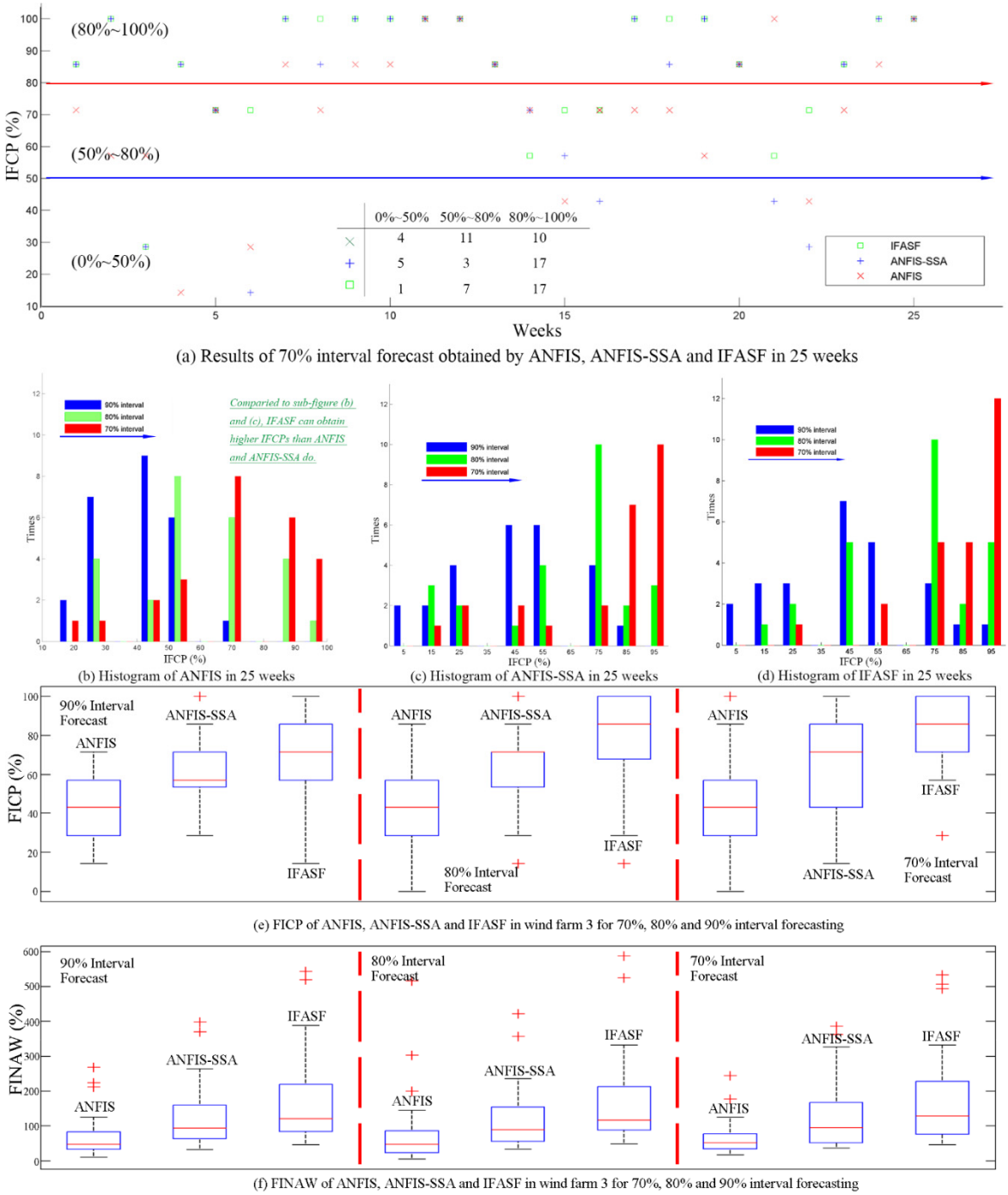

(a) Results of 70% interval forecast obtained by ANFIS, ANFIS-SSA and IFASF in 25 weeks

(b) Histogram of ANFIS in 25 weeks

(c) Histogram of ANFIS-SSA in 25 weeks

(d) Histogram of IFASF in 25 weeks

(e) FICP of ANFIS, ANFIS-SSA and IFASF in wind farm 3 for 70%, 80% and 90% interval forecasting

(f) FINAW of ANFIS, ANFIS-SSA and IFASF in wind farm 3 for 70%, 80% and 90% interval forecasting

Figure 11. Histograms and plots of the main results of the interval forecasts over 25 weeks in W3.

Table 6. Main interval forecasting results of ANFIS, ANFIS-SSA and IFASF in W3.

Weeks	ANFIS						ANFIS-SSA						IFASF					
	IFCP (%)			IFNAW (%)			IFCP (%)			IFNAW (%)			IFCP (%)			IFNAW (%)		
	90.00%	80.00%	70.00%	90.00%	80.00%	70.00%	90.00%	80.00%	70.00%	90.00%	80.00%	70.00%	90.00%	80.00%	70.00%	90.00%	80.00%	70.00%
1	42.86	71.43	71.43	28.82	49.93	68.96	42.86	71.43	85.71	25.24	47.04	68.13	42.86	71.43	85.71	27.04	47.81	68.44
2	42.86	57.14	57.14	43.07	117.98	166.96	57.14	71.43	100.00	84.22	150.44	208.02	42.86	71.43	100.00	70.16	132.64	188.77
3	42.86	42.86	57.14	24.62	40.36	66.97	28.57	14.29	28.57	8.99	36.07	77.19	28.57	28.57	28.57	35.62	51.67	76.54
4	28.57	28.57	14.29	26.12	46.82	61.99	28.57	71.43	85.71	5.49	63.09	93.86	14.29	42.86	85.71	28.49	51.97	76.27
5	57.14	85.71	71.43	71.03	111.75	88.75	42.86	57.14	71.43	33.24	95.48	167.80	71.43	71.43	71.43	62.05	96.46	133.03
6	42.86	28.57	28.57	224.02	398.30	543.54	71.43	14.29	14.29	515.93	89.52	138.06	42.86	71.43	71.43	73.86	326.57	493.48
7	71.43	71.43	85.71	268.52	263.36	388.73	71.43	100.00	100.00	144.50	235.77	332.51	57.14	100.00	100.00	125.58	239.55	332.19
8	57.14	71.43	71.43	112.06	180.12	231.92	28.57	57.14	85.71	76.97	176.41	263.09	42.86	71.43	100.00	117.15	181.48	254.13
9	28.57	57.14	85.71	44.58	72.33	101.24	42.86	57.14	100.00	47.65	81.81	116.76	42.86	42.86	100.00	42.60	81.00	116.97
10	57.14	85.71	85.71	125.02	214.97	302.33	71.43	100.00	100.00	113.43	198.82	277.79	71.43	100.00	100.00	99.18	194.24	276.53
11	57.14	100.00	100.00	211.39	369.57	519.13	85.71	85.71	100.00	200.31	356.51	525.20	85.71	100.00	100.00	177.27	362.61	506.80
12	28.57	71.43	100.00	66.76	119.23	167.82	0.00	28.57	100.00	49.83	112.32	204.12	0.00	42.86	100.00	72.06	117.04	203.84
13	57.14	57.14	85.71	39.77	67.50	94.22	57.14	85.71	85.71	36.41	59.52	92.11	57.14	71.43	85.71	45.92	59.65	95.26
14	28.57	42.86	71.43	42.44	76.38	106.24	57.14	71.43	71.43	37.49	74.94	111.06	71.43	85.71	57.14	37.46	75.61	103.43
15	14.29	28.57	42.86	10.12	32.07	46.31	0.00	14.29	57.14	19.46	37.67	54.41	0.00	14.29	71.43	16.81	36.65	46.37
16	14.29	85.71	71.43	14.93	41.67	60.03	28.57	28.57	42.86	14.40	33.26	48.72	14.29	42.86	71.43	18.63	36.94	56.87
17	28.57	57.14	71.43	81.34	101.97	155.20	57.14	71.43	100.00	55.24	93.76	160.18	57.14	71.43	100.00	58.73	103.58	141.15
18	42.86	71.43	71.43	70.80	130.53	157.59	42.86	71.43	85.71	59.85	95.46	115.55	42.86	71.43	100.00	52.73	93.67	128.05
19	42.86	57.14	57.14	64.84	203.08	310.47	71.43	71.43	100.00	302.35	421.78	587.16	100.00	100.00	100.00	244.05	386.23	533.63
20	42.86	71.43	85.71	34.96	47.16	63.78	14.29	71.43	85.71	24.26	41.16	64.07	28.57	85.71	85.71	26.44	47.86	68.36
21	28.57	57.14	100.00	12.86	90.24	108.98	42.86	57.14	42.86	21.75	33.45	60.34	28.57	42.86	57.14	23.33	41.60	58.35
22	28.57	28.57	42.86	47.19	86.03	120.46	57.14	71.43	28.57	22.84	75.75	113.24	57.14	71.43	71.43	51.11	96.14	130.95
23	42.86	57.14	71.43	46.51	69.13	93.71	14.29	42.86	85.71	36.06	72.25	105.74	14.29	28.57	85.71	37.78	57.58	107.11
24	42.86	85.71	85.71	89.84	153.37	215.94	42.86	100.00	100.00	90.88	167.52	226.72	42.86	100.00	100.00	90.97	162.37	219.25
25	57.14	57.14	100.00	53.84	93.58	129.33	57.14	71.43	100.00	67.09	101.36	134.12	57.14	71.43	100.00	51.15	95.29	124.91
Std.	14.47	20.00	22.21	67.45	97.52	138.17	22.71	25.71	26.76	112.05	98.13	137.47	25.19	24.99	18.66	52.91	102.09	144.13
Average	41.14	61.14	71.43	74.22	127.10	174.82	44.57	62.29	78.29	83.76	118.05	173.84	44.57	66.86	85.14	67.45	127.05	181.63

Next, this experiment will show the comparison results among ARIMA, BPNN, ELM, ARIMA-SSA, BPNN-SSA, ELM-SSA, ANFIS, ANFIS-SSA and IFASF in W3. Table 7 shows the main interval forecasting results of the nine models by three criteria. From this table, IFASF obviously has a higher mean IFCP than other models and has the lowest CWC among these nine models when forecasting the wind power interval. From the perspective of the interval forecasts' utility, 90% interval forecasts are still invalid because the highest IFCP of these models is 47.43%, which is far from the standard 75%. Thus, we still mainly discuss each model's effectiveness when forecasting 70% and 80% intervals in this experiment. For the ARIMA and ARIMA-SSA models, the highest IFCP peaks at 84% by using ARIMA pre-processed by SSA for 70% interval forecasts, and the lowest CWC is 379.94, which appears when forecasting the 70% interval using ARIMA-SSA.

Table 7. Main interval forecasting results of the nine models in W3.

Model	Criteria								
	Mean IFCP (%)			Mean IFNAW (%)			Mean CWC (%)		
	90.00%	80.00%	70.00%	90.00%	80.00%	70.00%	90.00%	80.00%	70.00%
ARIMA	36.57	62.86	72.57	60.03	125.84	172.12	731.61	782.03	1495.36
BPNN	38.29	55.43	66.29	70.45	130.18	147.11	465.93	725.17	1191.36
ELM	28.57	57.14	70.86	67.60	124.19	175.83	866.92	725.21	728.27
ANFIS	41.14	61.14	71.43	74.22	127.10	174.82	423.99	497.45	580.47
ARIMA-SSA	47.43	69.14	84.00	69.62	126.78	177.31	699.51	482.95	379.94
BPNN-SSA	39.43	59.43	77.14	70.80	129.26	180.24	704.34	424.26	324.41
ELM-SSA	34.29	62.29	81.71	70.61	127.82	181.16	719.75	366.71	277.05
ANFIS-SSA	44.57	62.29	78.29	83.76	118.05	173.84	431.65	421.26	406.83
IFASF	44.57	66.86	85.14	67.45	127.05	181.63	460.78	326.63	269.79

From the perspective of comparisons between BPNN and BPNN-SSA, BPNN-SSA's CWCs are 424.26 and 324.41, which are lower than the 725.17 and 1191.36 obtained by BPNN when forecasting 70% and 80% intervals, respectively, indicating that SSA lays a strong foundation to improve the interval forecasting effectiveness. Notably, the CWC criteria decrease by nearly 57% from the original model to the model pre-progressed by SSA. For other models, SSA can improve their original models' forecasting effectiveness for 70% and 80% interval forecasts. Thus, for the benchmark models, their original models' forecasting effectiveness can always be improved, especially for the 70% interval forecasts. Detailed 70% interval forecast results of each week are listed in Table 8 and the 80% interval forecast results are in Table 9. Specifically, based on Table 8, the ARIMA model has the highest CWC, 18990.21, in the 19th week, and the lowest CWC this model obtains is 90.63, which appears in the first week when forecasting the 70% interval. For the 80% interval forecasts which is listed in Table 9, the CWC of ARIMA peaks at 7312.76 in the sixth week and arrives at 65.17 in the 16th. In Table 8, it can be seen that for the BPNN model, its CWC has the maximum value, 15334.56, in week 11 when forecasting the 70% mean wind power interval. Alternately, this model provides the best forecast results in week 16 for the 70% interval forecasts. ELM has the best forecasting performance in week 16 when forecasting the 80% interval and has the worst performance in week 6 for the 70% interval forecasts. In week 16, ANFIS obtains the best forecasting effectiveness for the 70% interval forecasts, and the CWC of this model peaks at 6082.28 in week 6 when forecasting the 70% mean wind power interval. For the ARIMA-SSA model, 44.94 is the lowest CWC, obtained in week 20 when forecasting the 80% interval, and 2687.22 is the highest CWC calculated by this model in week 6 for the 80% interval. BPNN-SSA has the best forecasting performance in week 4 for the 70% interval forecasting and has the worst performance in week 6 for the 80% interval forecasts. In Table 9, The lowest CWC obtained by ELM-SSA is 45.38 when forecasting the 80% interval of the mean wind power in the first week. In the contrast, 1265.31 is the highest CWC calculated by this model in the 6th week for the 80% interval forecasts. For the ANFIS-SSA model, its CWC peaks at 3011.94 in week 6 when forecasting the 70% interval and arrives at 59.52 in week 13 when forecasting the 80% interval. IFASF, the model

developed by SSA and FA, has the best performance in week 20 for the 80% interval forecasts and has the worst performance in week 6 for the 70% interval forecasts. Regarding the effectiveness of SSA, it is obvious that each model's forecasting ability is improved when utilizing SSA to pre-process the original data: the ARIMA model is improved by 22.90%, 10.00% and 15.75%; the BPNN model is improved by 3.00%, 7.22% and 16.37%, respectively; the ELM model is improved by 19.57%, 9.01% and 15.31%, respectively; and ANFIS is improved by 7.7%, 1.88% and 9.60%, respectively. These results indicate that SSA always improves models' forecasting effectiveness, although SSA has different effects on different models.

Table 8. CWC of each method when forecasting the 70% interval in W3.

Weeks	Methods								
	ARIMA	**BPNN**	**ELM**	**ANFIS**	**ARIMA-SSA**	**BPNN-SSA**	**ELM-SSA**	**ANFIS-SSA**	**IFASF**
1	90.63	209.70	157.66	151.41	108.98	76.60	63.34	68.13	68.44
2	190.64	169.56	184.16	574.70	203.94	513.50	198.22	208.02	188.77
3	234.14	2480.27	483.51	230.52	245.94	344.01	486.97	863.73	856.51
4	274.81	836.33	421.82	1352.39	115.66	74.01	197.16	93.86	76.27
5	973.54	380.51	390.58	194.85	79.53	232.88	116.30	368.41	292.08
6	9741.61	4747.14	9690.88	6082.28	1264.97	1197.97	1121.23	3011.94	1083.44
7	256.68	269.19	279.63	388.73	273.30	312.02	307.72	332.51	332.19
8	172.96	516.14	730.95	509.18	179.50	225.05	206.94	263.09	254.13
9	210.76	216.13	211.24	101.24	92.34	109.03	116.12	116.76	116.97
10	254.69	633.15	286.85	302.33	261.47	261.24	285.40	277.79	276.53
11	504.27	15334.56	1152.26	519.13	423.16	507.54	503.94	525.20	506.80
12	157.48	165.68	176.88	167.82	132.58	183.80	387.01	204.12	203.84
13	112.30	86.54	95.33	94.22	104.53	197.16	91.34	92.11	95.26
14	123.86	298.76	213.59	233.25	123.06	133.23	500.34	243.84	356.00
15	117.37	81.57	118.86	277.33	98.49	135.08	211.25	187.30	101.80
16	132.38	53.68	61.41	131.80	71.17	247.46	166.31	291.77	124.86
17	184.70	149.20	307.81	340.75	189.81	146.35	327.42	160.18	141.15
18	148.57	130.90	277.36	345.99	112.57	134.35	130.50	115.55	128.05
19	18990.21	618.60	590.81	1068.67	487.85	603.13	776.15	587.16	533.63
20	620.36	96.80	133.63	63.78	59.85	158.47	62.84	64.07	68.36
21	121.53	163.35	397.71	108.98	148.17	127.08	67.88	361.33	200.86
22	3159.35	1653.66	1408.36	721.38	4034.42	1270.82	154.83	1267.22	287.51
23	161.75	167.99	89.09	205.74	219.26	301.58	106.71	105.74	107.11
24	301.40	203.71	220.01	215.94	318.38	190.71	210.63	226.72	219.25
25	147.99	120.79	126.45	129.33	149.52	427.25	129.78	134.12	124.91
Mean	1495.36	1191.36	728.27	580.47	379.94	324.41	277.05	406.83	269.79

Table 9. CWC of each method when forecasting the 80% interval in W3.

Weeks	Methods								
	ARIMA	**BPNN**	**ELM**	**ANFIS**	**ARIMA-SSA**	**BPNN-SSA**	**ELM-SSA**	**ANFIS-SSA**	**IFASF**
1	69.59	100.19	111.81	109.62	180.62	95.49	45.38	103.27	104.97
2	997.32	511.75	125.22	406.08	162.48	385.94	443.37	330.29	291.21
3	108.92	677.80	653.63	241.69	276.44	618.79	1177.15	786.93	578.20
4	168.28	1217.38	570.98	523.87	74.62	495.75	370.74	138.51	311.22
5	1033.46	456.96	917.12	111.75	179.07	479.68	484.38	328.64	211.77
6	7312.76	6626.16	6791.56	4457.09	2687.22	2272.72	1265.31	1953.03	716.99
7	214.60	229.63	202.65	578.21	201.95	225.25	229.35	235.77	239.55
8	284.89	1003.30	895.77	395.46	125.07	482.17	346.37	607.21	398.44
9	153.23	380.90	757.76	248.98	154.32	389.81	437.54	281.61	485.06
10	736.62	215.79	200.31	214.97	176.52	184.69	204.38	198.82	194.24
11	354.86	383.25	1252.93	369.57	302.06	788.67	350.94	356.51	362.61
12	113.09	117.27	268.01	261.78	91.03	648.67	470.72	1256.88	700.92
13	88.25	185.26	146.29	232.33	83.42	261.87	145.29	59.52	130.97
14	210.38	1772.65	413.64	457.38	209.92	374.83	402.55	164.52	75.61
15	134.26	717.79	264.59	358.83	97.99	418.43	441.00	821.77	799.49
16	65.17	350.80	44.89	41.67	51.62	166.67	144.72	372.22	221.23
17	827.65	233.74	226.75	350.98	650.05	189.15	232.91	205.85	227.42
18	121.38	498.14	199.93	286.57	198.87	180.46	549.18	209.59	205.65
19	1342.65	1035.12	1432.69	699.04	344.05	438.17	418.68	926.02	386.23
20	99.49	128.81	97.35	103.53	44.94	112.06	52.82	90.36	47.86
21	92.03	129.45	288.26	310.63	114.21	298.78	169.21	115.13	249.12
22	2445.81	511.83	1689.43	962.72	2625.09	108.80	161.15	166.32	211.08
23	293.01	291.88	139.37	237.95	409.28	404.46	271.39	432.68	644.37
24	2158.51	143.50	346.10	153.37	2399.31	292.04	139.99	167.52	162.37
25	124.53	209.92	93.20	322.11	233.49	293.10	213.28	222.53	209.22
Mean	782.03	725.17	725.21	497.45	482.95	424.26	366.71	421.26	326.63

Nevertheless, no matter which model (basic models or models pre-progressed by SSA) is considered, the IFASF model still is the best interval forecasting model when forecasting the 70% and 80% wind power intervals. In Figure 12a, which presents a boxplot of each model when forecasting the 70% and 80% intervals, the blue line represents the mean CWC of the 80% interval forecasts, and the red line represents the mean CWC of the 70% interval forecasts. From the perspective of the models' forecasting effectiveness, IFASF apparently outperforms the other models. Thus, from the above analysis of forecasting results, the developed model, IFASF, is the best interval forecasting model for the mean wind power points in the W3 wind farm.

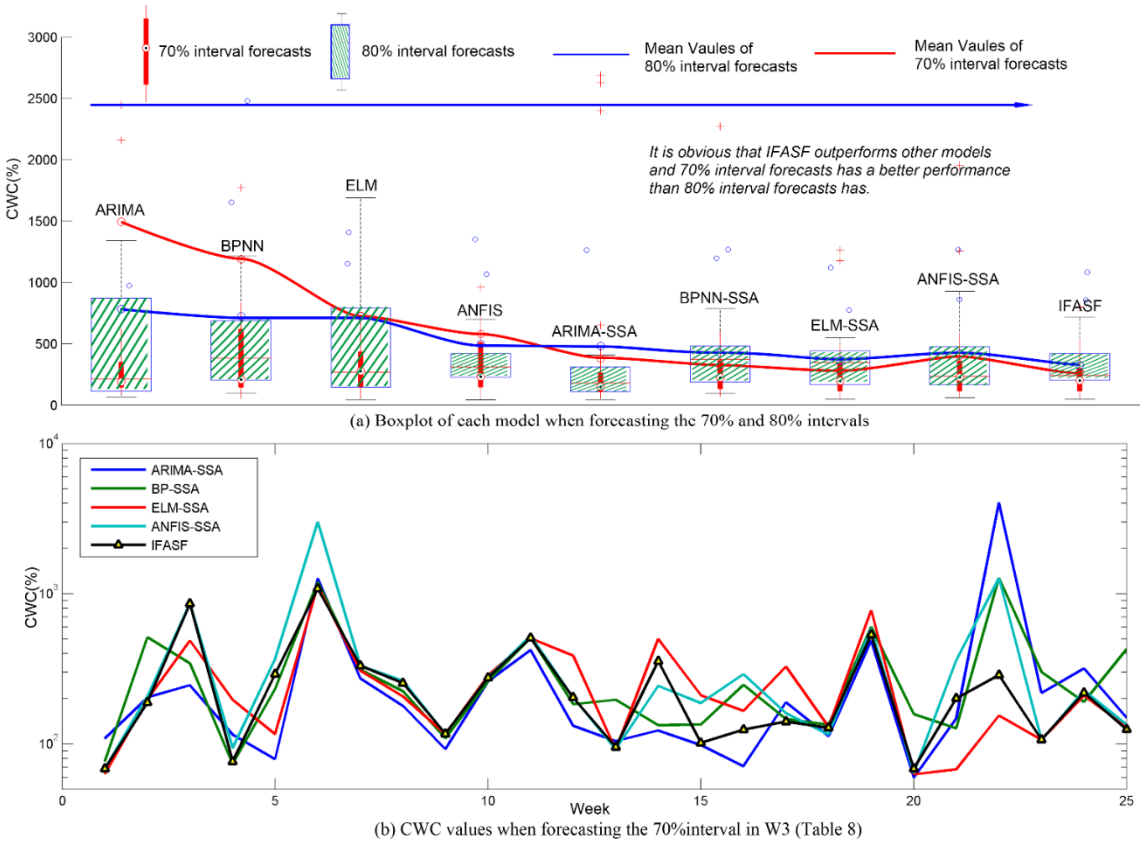

Figure 12. Boxplot of each model when forecasting the 70% and 80% intervals and illustration of Table 8.

From the results of these four experiments, it is apparent that IFASF is a good model to calculate the upper and lower bounds for these different wind farms, which means that the developed model has a good forecasting capability and good adaptability for mean wind power curves of different wind farms.

4.2.5. Experiment V

In this experiment, we will test the forecasting effectiveness of the proposed model for six-hour average wind power in three wind farms (W1, W2 and W3). The CWC results of nine models are listed in Table 10.

Table 10. CWC of each model when forecasting intervals of wind power in three wind farms.

Model	Wind Farms								
	W1			W2			W3		
	90.00%	80.00%	70.00%	90.00%	80.00%	70.00%	90.00%	80.00%	70.00%
ARIMA	514.59	434.21	488.56	726.49	828.66	927.34	485.97	368.13	529.38
BPNN	386.11	391.48	300.62	440.77	621.50	833.45	349.64	355.16	354.12
ELM	396.46	368.53	366.36	526.16	698.31	762.18	311.84	346.90	363.31
ANFIS	214.63	214.10	212.80	378.72	409.17	497.20	194.30	393.42	342.02
ARIMA-SSA	404.59	261.47	231.92	571.40	687.42	650.38	431.23	481.04	580.91
BPNN-SSA	189.57	214.58	222.81	197.44	189.36	212.37	200.85	216.30	224.94
ELM-SSA	205.91	185.60	175.48	190.72	219.87	247.88	204.53	171.13	181.34
ANFIS-SSA	206.43	197.97	200.39	206.43	197.97	200.39	195.02	204.60	200.68
IFASF	165.08	158.65	154.01	185.57	187.15	189.63	168.76	170.16	173.39

From Table 10, it can be seen that IFASF still outperforms other benchmarks by comparing CWC and the 90% interval forecasts have better performance than 80% and 70% interval forecasts in W2 and W3. The results show that the proposed model not only has a good performance of interval forecasts of daily average wind powers but also is suitable for six-hour average wind power, indicating that FA and SSA are effective for improving forecasting accuracy and can be used to optimize ANFIS to forecast the wind power's interval for different time horizons.

5. Conclusions

As wind energy has become increasingly important for the electrical market, effective forecast techniques are of great necessity for grid integration due to the unstable nature of wind. Based on a brief review of wind power forecast skills, this paper develops a hybrid model, IFASF, to provide intervals for future wind power points. Compared to the conventional prediction methods, the proposed model directly yields forecast intervals to avoid the accumulated error of deterministic prediction. Moreover, due to the inadequate research focusing on the daily average interval, the average value of wind power is emphasized in this paper to provide basic awareness of the potential wind energy in advance for both TSOs (Transmission System Operators) and IPPs (Independent Power Producers). This basic awareness is essential to increase profits for wind energy producers and maintain stability in electrical systems because the uncertainty forecast improves the capability of trouble prevention before electricity deficit (or redundancy).

Comprehensive comparisons are included here to validate the availability and stability of IFASF from 25 weeks of wind power data in Gansu, China. The superiority of IFCP, IFNAW and CWC highlight two improved aspects of this hybrid model, one demonstrating that SSA is an effective de-noising method for wind power series and the other demonstrating the favorable optimization ability of the FA. Furthermore, although 90% interval (when the confidence level α = 10%) forecasts have smaller interval widths, their coverage probability is very low. Therefore, to avoid unacceptable loss, a confidence level smaller than 10% is not suggested to be applied to wind power data, considering its sharp fluctuation. Because uncertainty forecasts of daily average wind power values have rarely been studied in the past, comparisons among methods in this paper provide a general reference for this aspect of statistical or artificially intelligent interval forecast methods. The comparison results are supported by the data validation from three wind farms, showing that the developed model improves on the original ARIMA, BPNN and ELM models by the average extents of approximately 63%, 61%, 56% for each method of 80% intervals and 67%, 69%, 49% for each method of 70% intervals. Thus, the hybrid model IFASF is suggested as an appropriate forecast model for daily wind power intervals in applications due to its satisfactory accuracy and the necessity of its application.

Acknowledgments: This work was supported by the National Key Technology Research and Development Program (2013BAB05B01).

Author Contributions: Zhongrong Zhang and Feng Liu designed experiments; Feng Liu and Yiliao Song carried out experiments; Feng Liu analyzed experimental results. Zhongrong Zhang analyzed sequencing data and developed analysis tools. Jinpeng Liu assisted with Illumina sequencing. Zhongrong Zhang, Yiliao Song and Feng Liu wrote the manuscript.

Conflicts of Interest: The authors declare no conflict of interest.

Acronyms

FA	Firefly Algorithm
SSA	Singular Spectrum Analysis
PCA	Principal Component Analysis
NWP	Numeric Weather Prediction
FIS	Fuzzy Inference System
ELM	Extreme Learning Machine
ANFIS	Adaptive-Network-Based Fuzzy Inference System
IFNAW	Interval Forecast Normalized Average Width
IFCP	Interval Forecast Coverage Probability
CWC	Coverage Width-based Criteria
BPNN	Back Propagation Neural Network
ARIMA	Autoregressive Integrated Moving Average Model

Appendix

$IFCP$ shows the coverage probability of target values between lower and upper limits with the following form [44]:

$$IFCP\left(y_i, \mathrm{U}_i, L_i\right) = \frac{1}{n}\sum_{i=1}^{n} I_{L_i \leqslant y_i \leqslant U_i}\left(y_i\right) \tag{A1}$$

where y_i is the real value, n denotes the sample size. U_i and L_i are separately the upper and lower prediction of y_i. $I_{L_i \leqslant y_i \leqslant U_i}\left(y_i\right)$ is the indicative function, equaling 1 if $L_i \leqslant y_i \leqslant U_i$ and 0 if not.

$IFNAW$ quantifies the normalized average width of the interval and is computed by the following formula [45]:

$$IFNAW = \frac{1}{nR}\sum_{i=1}^{n}\left(U_i - L_i\right) \tag{A2}$$

where R is the difference between the maximum and minimum values.

Based on the above two criteria, the coverage width-based criterion is proposed to summarize the interval forecasting ability including coverage probability and interval width. It is computed as follows [44,45]:

$$CWC = IFNAW \times \left\{1 + I_{IFCP<\mu}\left(IFCP\right)\exp\left(-\eta\left(IFCP - \mu\right)\right)\right\} \tag{A3}$$

where μ is determined by the nominal confidence level, while η is usually a large value to magnify the difference between $IFCP$ and μ. $I_{IFCP<\mu}\left(IFCP\right)$ denotes the indicator function and equals 1 if $IFCP < \mu$.

References

1. Ramirez-Rosado, I.J.; Fernandez-Jimenez, L.A.; Monteiro, C.; Sousa, J.; Bessa, R. Comparison of two new short-term wind-power forecasting systems. *Renew. Energy* **2009**, *34*, 1848–1854. [CrossRef]
2. National Energy Administration 2014. Available online: http://www.nea.gov.cn/2015-02/12/c_133989991.htm (accessed on 25 January 2016).
3. National Energy Administration 2015. Available online: http://www.nea.gov.cn/2015-06/08/c_134305870.htm (accessed on 25 January 2016).

4. Sideratos, G.; Hatziargyriou, N.D. Wind Power Forecasting Focused on Extreme Power System Events. *IEEE Trans. Sustain. Energy* **2012**, *3*, 445–454. [CrossRef]
5. Zhao, P.; Wang, J.; Xia, J.; Dai, Y.; Sheng, Y.; Yue, J. Performance evaluation and accuracy enhancement of a day-ahead wind power forecasting system in China. *Renew. Energy* **2012**, *43*, 234–241. [CrossRef]
6. Bhaskar, K.; Singh, S.N. AWNN-Assisted Wind Power Forecasting Using Feed-Forward Neural Network. *IEEE Trans. Sustain. Energy* **2012**, *3*, 306–315. [CrossRef]
7. Han, L.; Romero, C.E.; Yao, Z. Wind power forecasting based on principle component phase space reconstruction. *Renew. Energy* **2015**, *81*, 737–744. [CrossRef]
8. Traiteur, J.J.; Callicutt, D.J.; Smith, M.; Roy, S.B. A short-term ensemble wind speed forecasting system for wind power applications. *J. Appl. Meteorol. Climatol.* **2012**, *51*, 1763–1774. [CrossRef]
9. Silva, L. A feature engineering approach to wind power forecasting. *Int. J. Forecast.* **2014**, *30*, 395–401. [CrossRef]
10. Mahoney, W.P.; Parks, K.; Wiener, G.; Liu, Y.; Myers, W.L.; Sun, J.; Delle Monache, L.; Hopson, T.; Johnson, D.; Haupt, S.E. A Wind Power Forecasting System to Optimize Grid Integration. *IEEE Trans. Sustain. Energy* **2012**, *3*, 670–682. [CrossRef]
11. Croonenbroeck, C.; Dahl, C.M. Accurate medium-term wind power forecasting in a censored classification framework. *Energy* **2014**, *73*, 221–232. [CrossRef]
12. Karayiannis, N.B.; Member, S.; Randolph-gips, M.M. Probabilistic Wind Power Forecasting Using Radial Basis Function Neural Networks. *Power Syst. IEEE Trans.* **2003**, *14*, 835–846.
13. Kou, P.; Gao, F.; Guan, X. Sparse online warped Gaussian process for wind power probabilistic forecasting. *Appl. Energy* **2013**, *108*, 410–428. [CrossRef]
14. Bessa, R.J.; Miranda, V.; Botterud, A.; Wang, J. Time Adaptive Conditional Kernel Density Estimation for Wind Power Forecasting. *IEEE Trans. Sustain. Energy* **2012**, *3*, 660–669. [CrossRef]
15. Carpinone, A.; Giorgio, M.; Langella, R.; Testa, A. Markov chain modeling for very-short-term wind power forecasting. *Electr. Power Syst. Res.* **2015**, *122*, 152–158. [CrossRef]
16. Pinson, P. Very-short-term probabilistic forecasting of wind power with generalized logit—Normal distributions. *J. R. Stat. Soc. Ser.C Appl. Stat.* **2012**, 555–576. [CrossRef]
17. Bessa, R.J.; Miranda, V.; Botterud, A.; Zhou, Z.; Wang, J. Time-adaptive quantile-copula for wind power probabilistic forecasting. *Renew. Energy* **2012**, *40*, 29–39. [CrossRef]
18. Pinson, P.; Nielsen, H.A.; Madsen, H.; Kariniotakis, G. Skill forecasting from ensemble predictions of wind power. *Appl. Energy* **2009**, *86*, 1326–1334. [CrossRef]
19. Pinson, P.; Madsen, H.; Papaefthymiou, G. From Probabilistic Forecasts to Wind Power Production. *Production* **2009**, *12*, 51–62.
20. Qin, S.; Liu, F.; Wang, J.; Song, Y. Interval forecasts of a novelty hybrid model for wind speeds. *Energy Rep.* **2015**, *1*, 8–16. [CrossRef]
21. Jursa, R.; Rohrig, K. Short-term wind power forecasting using evolutionary algorithms for the automated specification of artificial intelligence models. *Int. J. Forecast.* **2008**, *24*, 694–709. [CrossRef]
22. Monteiro, C.; Bessa, R.; Miranda, V.; Botterud, A.; Wang, J.; Conzelmann, G. *Wind Power Forecasting: State-of-the-Art 2009 Decision and Information Sciences Division*; Argonne National Laboratory: Lemont, IL, USA, 2009; pp. 1–216.
23. Foley, A.M.; Leahy, P.G.; Marvuglia, A.; McKeogh, E.J. Current methods and advances in forecasting of wind power generation. *Renew. Energy* **2012**, *37*, 1–8. [CrossRef]
24. Sideratos, G.; Hatziargyriou, N.D. An Advanced Statistical Method for Wind Power Forecasting. *IEEE Trans. Power Syst.* **2007**, *22*, 258–265. [CrossRef]
25. Shi, J.; Ding, Z.; Member, S.; Lee, W.; Yang, Y.; Liu, Y.; Analysis, A.G.R. Hybrid forecasting model for very-short term wind power forecasting based on grey relational analysis and wind speed distribution features. *IEEE Trans. Smart Grid* **2014**, *5*, 521–526. [CrossRef]
26. Croonenbroeck, C.; Stadtmann, G. Minimizing asymmetric loss in medium-term wind power forecasting. *Renew. Energy* **2015**, *81*, 197–208. [CrossRef]
27. Broomhead, D.S.; King, G.P. Extracting qualitative dynamics from experimental data. *Phys. D Nonlinear Phenom.* **1986**, *20*, 217–236. [CrossRef]
28. Jang, J.R. ANFIS: Adaptive-Network-Based Fuzzy Inference System. *IEEE Trans. Syst. Man Cybern.* **1993**, *23*, 665–685. [CrossRef]

29. Yang, X. Firefly algorithms for multimodal optimization, in Stochastic Algorithms: Foundations and Applications (SAGA 2009). *Stoch. Algorithms Found. Appl.* **2009**, *5792*, 169–178.
30. Vautard, R.; Yiou, P.; Ghil, M. Singular-spectrum analysis A toolkit for short, noisy chaotic signals. *Phys. D Nonlinear Phenom.* **1992**, *58*, 95–126. [CrossRef]
31. Kondrashov, D.; Shprits, Y.; Ghil, M. Gap filling of solar wind data by singular spectrum analysis. *Geophys. Res. Lett.* **2010**, *37*, 1–6. [CrossRef]
32. Hsieh, W.W.; Hamilton, K. Nonlinear singular spectrum analysis of the tropical stratospheric wind. *Q. J. R. Meteorol. Soc.* **2003**, *129*, 2367–2382. [CrossRef]
33. Takens, F. Detecting strange attractors in turbulence. *Dyn. Syst. Turbul. Warwick 1980* **1981**, *898*, 366–381.
34. Liu, Y.-F.; Zhao, M. De-Noising of Chaotic Time Series Based on Singular Spectrum Analysis. *J. Shanghai Jiaotong Univ.* **2003**, *37*, 778–780.
35. Mohandes, M.; Rehman, S.; Rahman, S.M. Estimation of wind speed profile using adaptive neuro-fuzzy inference system (ANFIS). *Appl. Energy* **2011**, *88*, 4024–4032. [CrossRef]
36. Pousinho, H.M.I.; Mendes, V.M.F.; Catalão, J.P.S. A hybrid pso-anfis approach for short-term wind power prediction in Portugal. *Energy Convers. Manag.* **2011**, *52*, 397–402. [CrossRef]
37. Takagi, T.; Sugeno, M. Fuzzy identification of systems and its applications to modeling and control. *IEEE Trans. Syst. Man Cybern.* **1985**, *SMC-15*, 116–132. [CrossRef]
38. Hiremath, S.M.; Patra, S.K.; Mishra, A.K. Extended date rate prediction for cognitive radio using ANFIS with Subtractive Clustering. In Proceedings of the 2012 5th International Conference on Computers and Devices for Communication (CODEC), Kolkata, Calcutta, 17–19 December 2012.
39. Chiu, S.L. Fuzzy Model Identification Based on Cluster Estimation. *J. Intell. Fuzzy Syst.* **1994**, *2*, 267–278.
40. Chen, M.Y. A hybrid ANFIS model for business failure prediction utilizing particle swarm optimization and subtractive clustering. *Inf. Sci.* **2013**, *220*, 180–195. [CrossRef]
41. Yu, J.; Chen, K.; Mori, J.; Rashid, M.M. A Gaussian mixture copula model based localized Gaussian process regression approach for long-term wind speed prediction. *Energy* **2013**, *61*, 673–686. [CrossRef]
42. Wan, C.; Xu, Z.; Pinson, P. Direct interval forecasting of wind power. *IEEE Trans. Power Syst.* **2013**, *28*, 4877–4878. [CrossRef]
43. Geng, J.; Huang, M.; Li, M.; Hong, W. Neurocomputing Hybridization of seasonal chaotic cloud simulated annealing algorithm in a SVR-based load forecasting model. *Neurocomputing* **2015**, *151*, 1362–1373. [CrossRef]
44. Quan, H.; Srinivasan, D.; Khosravi, A. Short-term load and wind power forecasting using neural network-based prediction intervals. *IEEE Trans. Neural Netw. Learn. Syst.* **2014**, *25*, 303–315. [CrossRef] [PubMed]
45. Khosravi, A.; Nahavandi, S.; Creighton, D. Prediction intervals for short-term wind farm power generation forecasts. *IEEE Trans. Sustain. Energy* **2013**, *4*, 602–610. [CrossRef]